

UDK 621.315.592

Gallium vacancy — shallows donor complexes in *n*-GaAs doped with elements of group VI Te or S (Review)

© A.A. Gutkin, N.S. Averkiev[†]

Ioffe Institute,
194021 St. Petersburg, Russia

[†]E-mail: Averkiev@les.ioffe.ru, agut.defect@mail.ioffe.ru

Received September 6, 2022

Revised October 26, 2022

Accepted October 26, 2022.

The results of studies of Ga vacancy (V_{Ga}) — shallow donor (Te or S atom substituting As atom in the lattice site closest to the vacancy) complexes by methods of photoluminescence under resonant polarized excitation and piezospectroscopy are considered. An analysis of the experimental data in the classical dipole approximation shows that the symmetry of the complexes is lower than the trigonal one and their optical properties are explained in the model of a monoclinic defect with a symmetry plane of the $\{011\}$ type, in which the initial trigonal axis and the axis of the optical dipole lie. The reason for the lowering of the symmetry of the initially trigonal center is the distortions arising from the Jahn-Teller effect. A microscopic model is proposed that relates the behavior peculiarities of the optical properties of the $V_{\text{Ga}}\text{Te}_{\text{As}}$ complex under uniaxial deformations and temperature changes with the structure of the electronic levels and the change in the charge state of the complex. The differences in this behavior observed for the $V_{\text{Ga}}\text{S}_{\text{As}}$ complex are analyzed and possible reasons for their appearance are discussed.

Keywords: vacancy complexes in GaAs, Jahn-Teller effect, photoluminescence under resonant excitation, piezospectroscopy.

DOI: 10.21883/SC.2022.11.54956.9957

1. Introduction

Isolated intrinsic point defects and complexes with their participation create centers with deep levels in semiconductors and can significantly affect the properties of the material. Studies of these centers are carrying out for a long time (see, for example, [1–5]).

Complexes of this type, containing a vacancy and a shallow donor and leading to the formation of deep acceptor levels in the forbidden band, were first identified and studied in ZnS [6–9] and Si [10–13].

The assumption that a broad photoluminescence band with a maximum at a photon energy of about 1.2 eV in *n*-GaAs is associated with Ga vacancy (V_{Ga}) — donor complexes and is caused by electron transitions from a shallow donor-like state to the ground state of the complex, was done in 1968 [14,15]. This assumption was based mainly on the absence of the indicated luminescence band in crystals grown from solutions in Ga (i.e., practically free of V_{Ga}) [16,17], and by shift, observed in paper [14], of the maximum position of the luminescence band by ~ 0.02 eV, when doping with donors of the VI group (Te_{As} , Se_{As} , S_{As}) was replaced by doping with donors of IV group (Sn_{Ga} , Ge_{Ga} , Si_{Ga}). A similar shift associated with different positions of the donor relative to the vacancy was previously discovered in paper [18] for the emission band of Zn vacancy — shallow donor complexes in ZnS, the spatial structure and composition of which were confirmed

by optical experiments [8] and paramagnetic resonance studies [9]. Other properties of the indicated emission bands of the complexes in ZnS and GaAs turned out to be similar. The change in the photoluminescence band width with temperature was well described by a one-dimensional configuration-coordinate diagram, suggesting a strong interaction with phonons, whose energy for the $V_{\text{Ga}}\text{Sn}_{\text{Ga}}$ complexes turned out to be 22 meV. For some complexes in GaAs ($V_{\text{Ga}}\text{Ge}_{\text{Ga}}$, $V_{\text{Ga}}\text{Sn}_{\text{Ga}}$, $V_{\text{Ga}}\text{Si}_{\text{Ga}}$), as well as for complexes in ZnS [8], the resonant excitation of this radiation was observed, the long-wavelength boundary of which was noticeably below the threshold of the intrinsic absorption band of GaAs [15,19]. This was an additional substantiation of the proposed model of the complex in GaAs [14,15].

In further studies [20–25], related to the properties of the luminescence band with a maximum of about 1.2 eV in *n*-GaAs:Te, upon excitation by light from the intrinsic absorption band (i.e., due to the generation of free electrons and holes) this radiation, as in [14,15], was associated with V_{Ga} — shallow donor (Te_{As}) complexes. Small variations in the shape and position of the maximum of this band in different samples were found in [21,22], which were explained by changes in the vibrational properties and energy levels of these complexes under the influence of other defects located near them. The energy of local phonons, obtained, as in the papers [14,15], from the analysis of the temperature dependence of the photoluminescence band

width, turned out to be different for various samples and was in the range of 17–21 meV. In paper [23] it was found that, although holes are captured by the complex almost instantaneously, the characteristic photoluminescence decay time is relatively large and decreases with the electron concentration increasing. Its value for electron concentrations $10^{17}–10^{18} \text{ cm}^{-3}$ is in the range 2–0.5 μs . At the same time, it was concluded that in the case of a high concentration of electrons in the illuminated sample, the radiation is practically determined by the transitions of electrons from *c*-band to the ground state of the complex, while in the case of low concentration of free electrons the radiation can significantly be determined by the transitions of electrons previously captured on a shallow donor state [23].

The interaction of intrinsic defects and donor impurities during the growth of crystals *n*-GaAs:Te and *n*-GaAs:Sn was considered in papers [26,27]. The analysis of the experimental results carried out in these papers showed that the formation of a sufficiently large number of V_{Ga} — shallow donor complexes can explain the partial compensation of donors observed in these crystals, as well as the dependence of the shallow donors concentration on Te concentration in the melt, and superexpansion of the lattice in GaAs:Te.

Thus, studies carried out by the beginning of the 80s of the last century confirmed both the existence of stable complexes V_{Ga} — shallow donor in *n*-GaAs, and their role in luminescence with a maximum of about 1.2 eV. However, no direct determination of the spatial structure of the center associated with this band was implemented. Also, it was not studied the possible difference in the properties of these centers, when one shallow donor is replaced by another from elements of the same group. Such studies were carried out later, and in the case of doping GaAs with elements of group VI are considered in this review. At the same time, the analysis of experimental data in the classical dipole approximation was performed again, and errors, inaccuracies, and misprints were corrected. This resulted in change in the estimates of some parameters of the complexes, but did not change the qualitative conclusions.

Also note that the effects caused by cation-vacancy–donor complexes were also observed in some other semiconductors $A^{\text{III}}B^{\text{V}}$ [1] and in ZnO:Al [28]. One of the luminescence bands in GaN:Be [29] was bound with similar complex anion vacancy — acceptor $\text{Be}_{\text{Ga}}V_{\text{N}}$. However, the spatial structure of the complexes in these materials was not studied experimentally.

2. Complexes vacancy $V_{\text{Ga}}\text{Te}_{\text{As}}$

2.1. Photoluminescence excitation spectrum and study of optical anisotropy of complex by polarization spectroscopy method

One of the methods for determining the spatial symmetry of local centers in crystals is the polarization spectroscopy of photoluminescence, i.e., the study of the polarization of light emitted by the center under resonant polarized

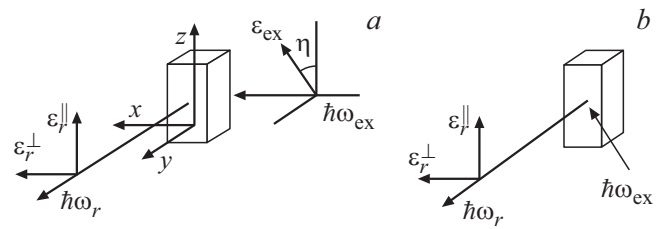


Figure 1. Schemes of optical experiments in studies of the anisotropy of impurity centers [34]. *a* — orthogonal scheme, *b* — scheme „on reflection“. ε_{ex} , $\varepsilon_r^{\parallel}$ and ε_r^{\perp} — electric vectors of the light wave of the exciting and emitted light.

excitation [30–32]. This method, in contrast to the photoluminescence excitation due to the generation of electron-hole pairs by light from the intrinsic absorption band of the semiconductor, requires the existence of direct excitation of the center due to the absorption by it of the photon, the energy of which is noticeably lower than the intrinsic absorption threshold of the crystal. In this case, various relative orientations of the exciting and measured emitted light beams are possible.

In the case of studying the photoluminescence polarization under polarized resonant excitation, it is convenient to use the orthogonal scheme of the experiment [30,31], when the direction of the observed photoluminescence is perpendicular to the direction of the exciting light (Fig. 1, *a*), which is oriented along one of the crystallographic axes of the sample under study. The degree of linear polarization ρ of luminescence at different angles η between the axis perpendicular to the directions of observation and excitation of luminescence and the direction of the electric vector of a linearly polarized exciting light wave is determined according to the expression

$$\rho(\eta) = \frac{I_{\parallel}(\eta) - I_{\perp}(\eta)}{I_{\parallel}(\eta) + I_{\perp}(\eta)}, \quad (1)$$

where I_{\parallel} and I_{\perp} are the photoluminescence intensities (the number of emitted photons) measured respectively at the direction of the electric vector of the emitted light shown in Fig. 1, *a*. When measuring the full excitation spectrum of impurity luminescence, which includes regions of strong light absorption, it is convenient to use the scheme „on reflection“ (Fig. 1, *b*). The same scheme was used in studies of the radiation polarization under uniaxial pressure and the generation of electron-hole pairs by light from the intrinsic absorption region of the semiconductor. In this case, the photoluminescence intensities were determined with electric light parallel and perpendicular to the pressure axis.

For the emission band with a maximum at about 1.2 eV in *n*-GaAs:Te, the resonant excitation was first observed in paper [33]. In more detail, the excitation spectra, i.e., the dependences of the photoluminescence intensity I_0 near its maximum ($\hbar\omega_r \approx 1.2 \text{ eV}$) on the photon energy of the

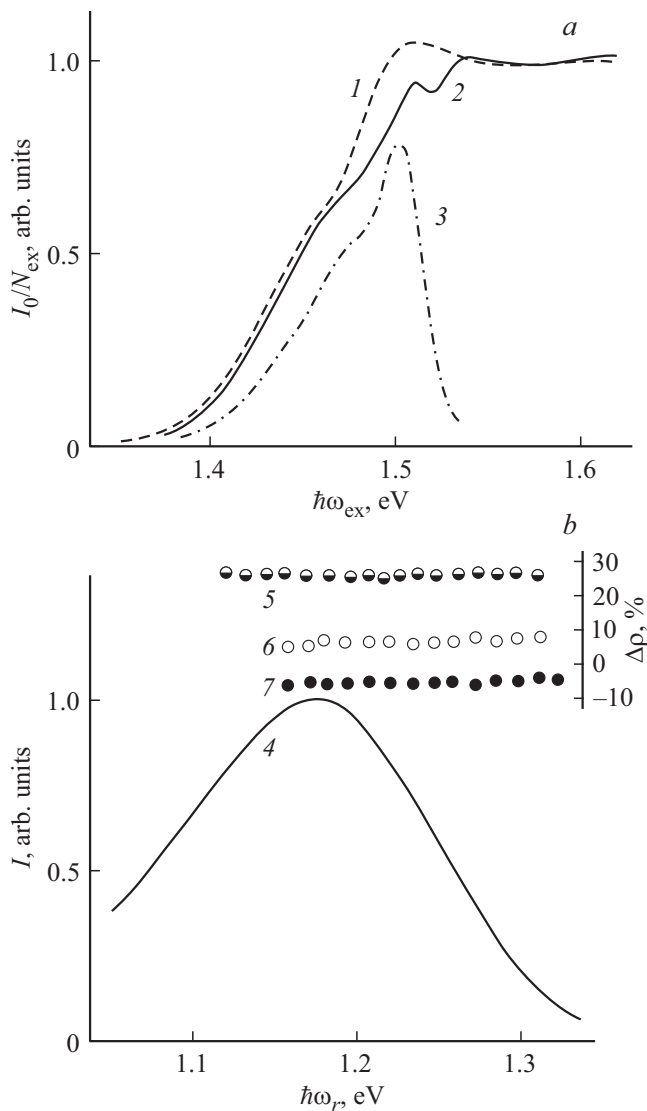


Figure 2. Photoluminescence of $V_{\text{Ga}}\text{Te}_{\text{As}}$ complexes in *n*-GaAs:Te [34]. *a* — photoluminescence excitation spectrum at $\hbar\omega_r \approx 1.2$ eV; *b* — photoluminescence spectrum and $\Delta\rho$ at $\hbar\omega_{\text{ex}} = 1.43$ eV. *T*, K: 1, 3–7 — 77, 2 — 4.2. 1, 2 — experimental scheme „on reflection“. 3–7 — orthogonal scheme of the experiment, directions of propagation of the exciting (indicated first) and observed emitted light: 5 — [011]–[100], 6 — [100]–[010], 7 — [110]–[1 $\bar{1}$ 0].

exciting light $\hbar\omega_{\text{ex}}$ reduced to an equal number of exciting photons (I_0/N_{ex}) were measured in paper [34]. These spectra, along with the spectrum of the photoluminescence band itself, are shown in Fig. 2. The samples for the study were cut from single crystals of *n*-GaAs obtained by the Czochralski method and doped with Te during growth. As can be seen from Fig. 2 (curves 1 and 2), the long-wavelength edge of the excitation spectrum of the studied photoluminescence at low temperature lies significantly below the threshold of intrinsic and exciton absorption and is at the photon energy $\hbar\omega_{\text{ex}} < 1.4$ eV.

Experimental dependences of $\Delta\rho = \rho(\eta=0) - \rho(\eta=90^\circ)$ on the energy of emitted and exciting photons ($\hbar\omega_r$ and $\hbar\omega_{\text{ex}}$, respectively) for various combinations of propagation directions of the exciting and emitted light in the orthogonal scheme of measurements, obtained on *n*-GaAs:Te samples with electrons concentration $n_0 \approx 5 \cdot 10^{17} \text{ cm}^{-3}$ are shown in Fig. 2, *b* and 3. These data, together with the results shown in Fig. 2*a*, indicate that significant contribution to the excitation of the studied luminescence at $\hbar\omega_{\text{ex}} \lesssim 1.5$ eV give resonant optical transitions. At the same time, since the value of $\Delta\rho$, within the measurement error, dependence on $\hbar\omega_{\text{ex}}$ stops for $\hbar\omega_{\text{ex}} \lesssim 1.43$ eV (Fig. 3), we can assume that the luminescence excitation in the case of $\hbar\omega_{\text{ex}} \lesssim 1.43$ eV corresponds to only one type of optical transition, namely, the electron transition from the highest filled energy level of the center. As the wavelength of the exciting light decreases (in the case of $\hbar\omega_{\text{ex}} \gtrsim 1.46$ eV for $T = 77$ K and $\hbar\omega_{\text{ex}} \gtrsim 1.48$ eV for $T = 4.2$ K) there is a rapid decrease in the absolute value $\Delta\rho$, followed by a sign change of $\Delta\rho$ (at least for the experimental configurations shown in Fig. 3, *a–c*). This behavior of $\Delta\rho$ may indicate the photoluminescence excitation due to optical transitions of electrons from a deeper level of the center. The emission band did not change in this case. Resonant optical transitions to this state also manifest themselves as a feature of the excitation spectrum near $\hbar\omega_{\text{ex}} \approx 1.5$ eV (Fig. 2, *a*). In some samples, this feature of the excitation spectra, and sometimes the sign change of $\Delta\rho$, was not observed. Apparently, this is due to differences in the ratio of resonant and interband (nonresonant) excitation near the fundamental absorption edge in different samples, which is due to the differences in the edge tailing of the main absorption band and by the concentrations of the studied complexes.

Also note that the constancy of $\Delta\rho$ over the emission spectrum (Fig. 2, *b*) may mean that the dominant contribution to the luminescence band width comes from the interaction with phonons that do not change the symmetry of the emitting center.

Fig. 4 shows the dependences of the degree of luminescence polarization on the position of the exciting light polarization plane $\rho(\eta)$ (polarization diagrams) upon excitation of electrons from the highest-energy filled state of the complex.

For a qualitative analysis of polarization spectroscopy data, the paper [34] used the usual approach [30–32], considering an anisotropic center as a superposition of a classical dipole linear oscillator and a rotator having a common axis. The relative contribution to the emission and absorption of the linear oscillator and a rotator can be different. The axes of oscillators that absorb and emit light can coincide (one-dipole approximation) or differ (two-dipole approximation), and all equivalent directions of these axes in a crystal are equally probable.

Calculations of polarization diagrams in such a model were carried out for various combinations of the directions of the axes of the emitting and absorbing dipoles along the principal axes of the crystal [34]. Comparison of the

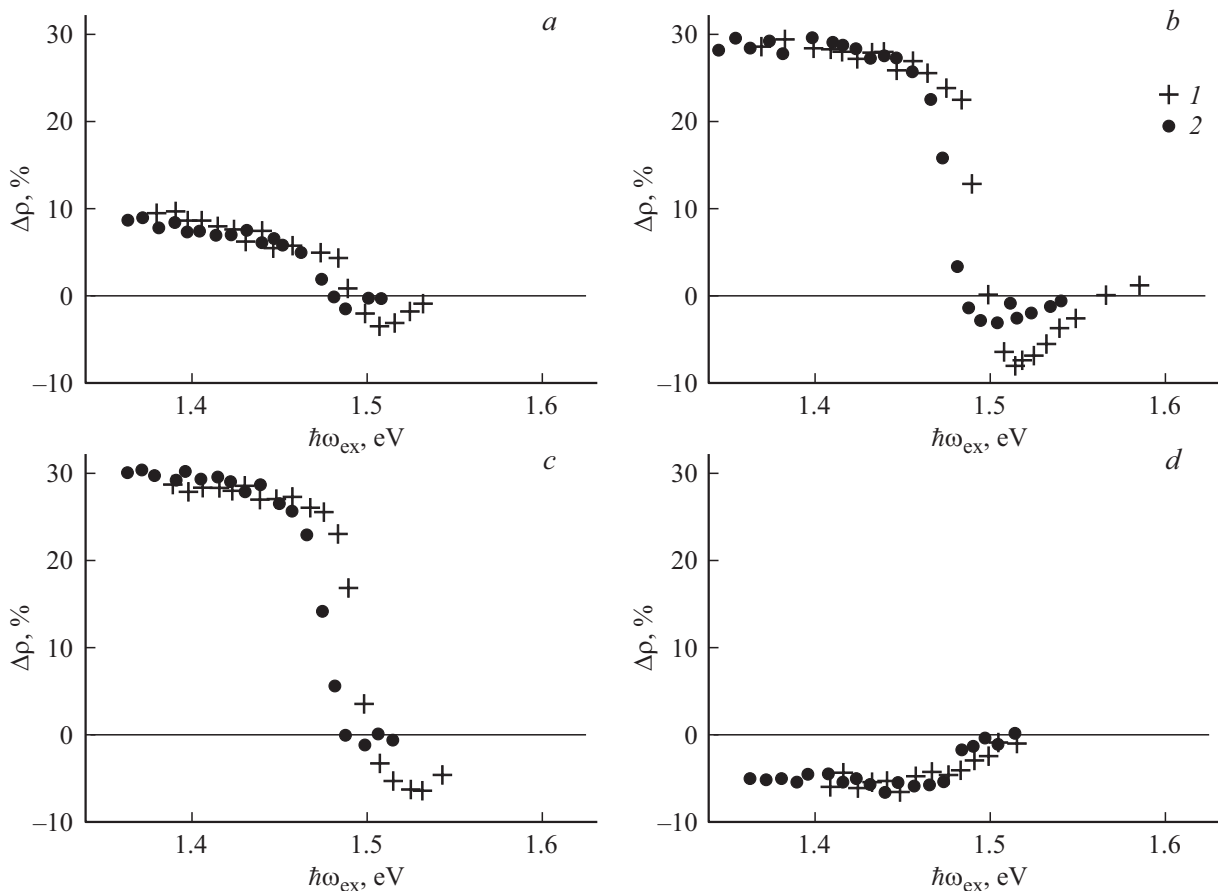


Figure 3. Difference in the degrees of photoluminescence polarization $\Delta\rho = \rho(\eta = 0) - \rho(\eta = 90^\circ)$ vs. photon energy of exciting light [34]. $\hbar\omega_r \approx 1.2$ eV. T, K : 1 — 4.2, 2 — 77. Orientation of directions of exciting (indicated first) and observed emitted light: a — $[100]-[010]$, b — $[100]-[011]$, c — $[110]-[001]$, d — $[110]-[1\bar{1}0]$.

results of these calculations with the experimental data presented in Fig. 4 showed that the axis of the emitting dipole cannot be parallel to the axes C_4 , C_3 , or C_2 , and the axis of the absorbing dipole cannot be parallel to axes C_4 or C_3 . In particular, for example, the existence of a nonzero projection of the axis of the emitting dipole onto the axis C_3 indicates the $\rho(\eta)$ increasing as η changes from 0 to 90° in Fig. 4, *d*, while the non-zero value $\rho(0)$ in the diagrams in Fig. 4, *a* and *d* indicates that the dipole axis also has a component that does not coincide with the same axis C_3 . Since, in the case of the existence of a preferred axis of an anisotropic center, the axis of the optical dipole [30–32] must coincide with this axis, this means that the complex under study does not have trigonal symmetry either during emission or absorption of light (the preferred axis of symmetry C_3), as one would expect for the complex that includes V_{Ga} and Te_{As} located strictly at neighboring lattice sites, and their undistorted environment of atoms crystal.

Note that the measurements carried out in the paper [33] at a temperature of 77 K and only for experimental configurations similar to those shown in Fig. 3 and 4, *a–c*, did not find the existence of polarization of the studied

photoluminescence in the case corresponding to Fig. 3, *a* and 4, *a*. Based on this, an erroneous conclusion was made about the trigonal symmetry of this center [33]. However, resonant excitation of photoluminescence in [33] was carried out at photon energy of 1.48 eV, which is close to the interband absorption edge and corresponds exactly to the region of the spectrum in which the induced polarization is close to 0 (Fig. 3). The significant influence of this circumstance on the decrease in the degree of induced polarization is also confirmed by the fact that the maximum values of $\rho(\eta)$ obtained in [33] for other experimental configurations were significantly lower than those obtained at $\hbar\omega_{ex} = 1.43$ eV (Fig. 4).

As shown in [34], the polarization diagrams corresponding to the excitation of a low-energy radiating state (Fig. 4) can be explained in terms of the two-dipole approximation for a center that in both absorbing and emitting states has the same plane of symmetry of type $\{110\}$ containing an axis connecting V_{Ga} and Te_{As} (the center of monoclinic symmetry C_s). The number of different orientations of such center in the crystal is 12. Quantitative calculations [34], confirming the above structure of the center, were carried out in the simplest model, which assumes that the initial

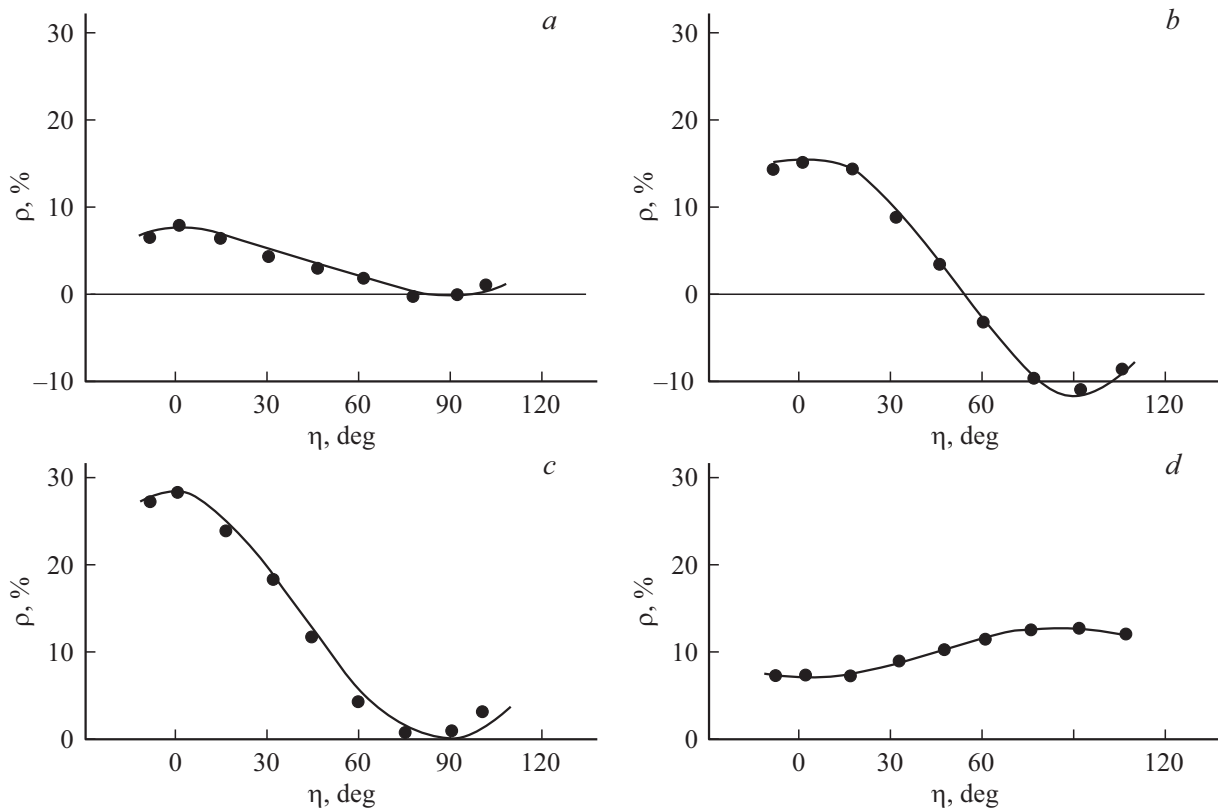


Figure 4. Polarization photoluminescence diagrams of $V_{\text{Ga}}\text{Te}_{\text{As}}$ complexes in *n*-GaAs:Te. ($n_0 \approx 5 \cdot 10^{17} \text{ cm}^{-3}$) [34]. $T = 77 \text{ K}$. $\hbar\omega_{\text{ex}} = 1.43 \text{ eV}$, $\hbar\omega_r \approx 1.2 \text{ eV}$. The orientation of the directions of the exciting and observed emitted light in Fig. *a, b, c* and *d* is the same as in Fig. 3. Dots — experiment, curves — calculation.

wave functions have *s*-type symmetry in the ground state, and in the emitting state — *p*-type. Distortions of the point symmetry of the center in both states were taken into account as a superposition of distortions along the axis $V_{\text{Ga}}\text{—Te}_{\text{As}}$ (axis $\langle 111 \rangle$) and one of the other principal axes of the crystal ($\langle 110 \rangle$ or $\langle 001 \rangle$). The influence of these distortions was simulated by introducing energy splittings of the excited state at the moment of excitation (δ_{111}^{ex} and δ_{110}^{ex} or δ_{001}^{ex}) and at the time of emission (δ_{111}^{r} and δ_{110}^{r} or δ_{001}^{r}), which is similar to splitting under uniaxial deformation along the corresponding axes. The influence of the spin-orbit interaction on the excited state was also taken into account.

The reasons for the lowering of the initially trigonal symmetry of the complex, as it was supposed in paper [34], may be the association with the pair $V_{\text{Ga}}\text{—Te}_{\text{As}}$ of one more defect or additional distortions due to the Jahn-Teller effect in the trigonal complex.

2.2. Effect of uniaxial pressure on the photoluminescence band with maximum near 1.2 eV in GaAs:Te and the spatial structure of the complex $V_{\text{Ga}}\text{—Te}_{\text{As}}$

The difference between the point symmetry of $V_{\text{Ga}}\text{Te}_{\text{As}}$ complex and the trigonal symmetry should also lead to characteristic features in the behavior of its photolumines-

cence under uniaxial deformation. Similar studies were carried out at uniaxial pressures P up to 10 kbar in papers [35–37]. The experiments were carried out in the scheme „on reflection“ (Fig. 1, *b*) with luminescence excitation due to the generation of electron-hole pairs by light from the intrinsic absorption band of GaAs (radiation of He—Ne laser, wavelength $0.6328 \mu\text{m}$). It was measured the spectra of the photoluminescence polarized parallel or perpendicular to the pressure axis ($I_{\parallel}(\hbar\omega_r)$ and $I_{\perp}(\hbar\omega_r)$, respectively), the polarization ratio of radiation relative to the pressure axis at different photon energies

$$r = I_{\parallel}(\hbar\omega_r)/I_{\perp}(\hbar\omega_r) \quad (2)$$

and integral polarization ratio of the radiation band, defined as

$$r^* = \frac{\int I_{\parallel}(\hbar\omega_r) d\hbar\omega_r}{\int I_{\perp}(\hbar\omega_r) d\hbar\omega_r}. \quad (3)$$

The samples for the study were made from the same single crystals as those used in the study of the complexes by the method of polarization spectroscopy [34]. Under the experimental conditions, the photoluminescence intensity was proportional to the intensity of the exciting light, and the degree of emission polarization did not depend on it. At $P = 0$ and low temperatures, r^* and r were equal to 1, which indicated the equally probable distribution of

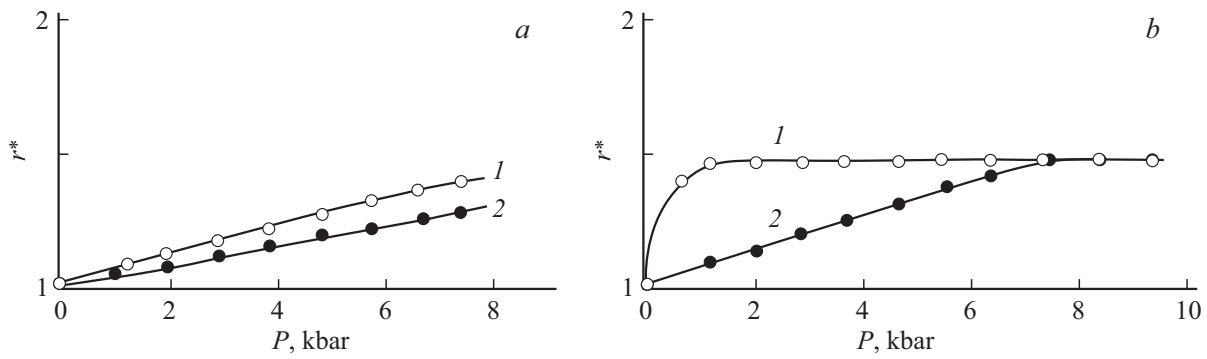


Figure 5. Experimental dependences of the polarization ratio of photoluminescence in the band with a maximum at photon energy ~ 1.2 eV on the uniaxial pressure [36]. Pressure direction: *a* — $[001]$, *b* — $[111]$. Photoluminescence excitation by light from intrinsic absorption band. *T*, K: 1 — 2, 2 — 77.

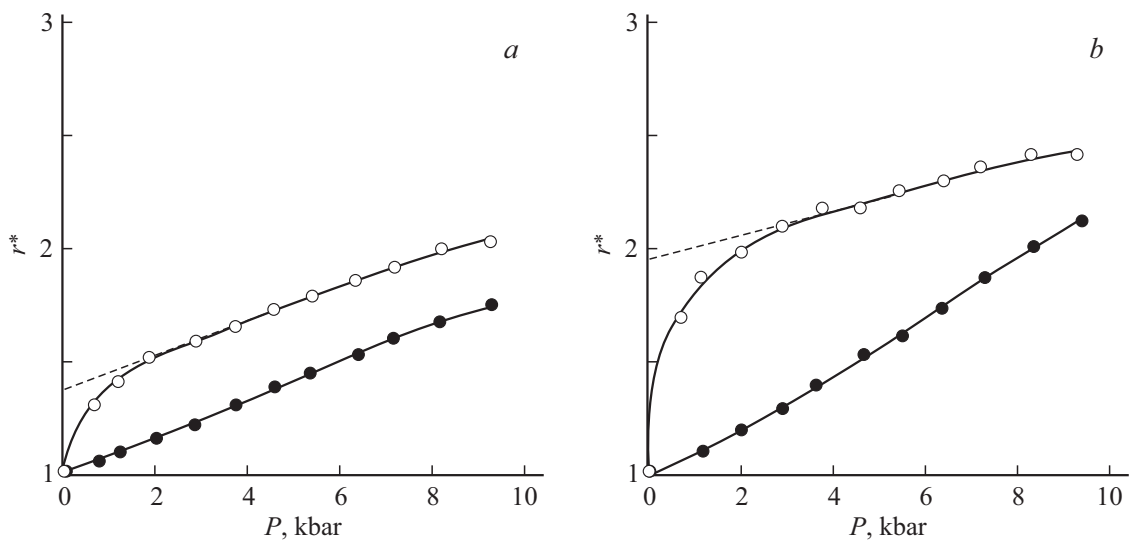


Figure 6. Experimental dependences of the polarization ratio of photoluminescence in the band with a maximum at photon energy ~ 1.2 eV on the uniaxial pressure [36]. Pressure direction $[110]$. Direction of photoluminescence observation: *a* — $[1\bar{1}0]$ and *b* — $[001]$. *T*, K: 1 — 2, 2 — 77. Photoluminescence excitation by light from the intrinsic absorption band of GaAs.

complexes over all possible orientations of the axes of pair $V_{\text{Ga}}\text{--Te}_{\text{As}}$ and directions of additional distortions of the emitting state.

It was shown that the integral polarization ratio of the emission band increased in the case of uniaxial compression, and this increasing at temperature of 77 K was smaller than at 2 K. This indicates that, in addition to the simple removal of the orientational degeneracy of different centers (see, for example, [38]), other processes also take place.

The dependences of r^* on the value of the applied uniaxial pressure for its different directions are presented in Fig. 5 and 6 [36]. A characteristic feature of these dependences at $P \parallel [111]$ or $P \parallel [110]$ and temperature 2 K is a rapid stepwise increasing of the polarization ratio with P increasing in the region of low pressures, followed by more slow increasing in the pressure range 2–10 kbar. At the same time, at $T = 77$ K, the polarization ratio of the radiation grows smoothly over the entire studied pressure range. Such a behavior of the photoluminescence

polarization of the local center of monoclinic symmetry under uniaxial pressure can be explained by the existence of several possible and equivalent at $P = 0$ configurations for each individual center, caused by distortion associated with the Jahn-Teller effect (i.e., with the interaction of bound carriers with nontotally symmetric vibrations of the complex atoms). Uniaxial pressure causes differences in the energy levels of these configurations of the individual center due to the different orientation of the Jahn-Teller distortions with respect to the pressure axis. This leads to a difference in the equilibrium concentrations of various configurations of the complex, i.e., to partial or complete alignment of distortions in equilibrium due to their spontaneous reorientation. The latter causes the appearance of emission polarization of the entire set of complexes, as in the case of polarized resonant excitation, when the probability of excitation of complexes of various configurations is different. Another possible mechanism for distortions alignment is the pressure influence on the probability of the various

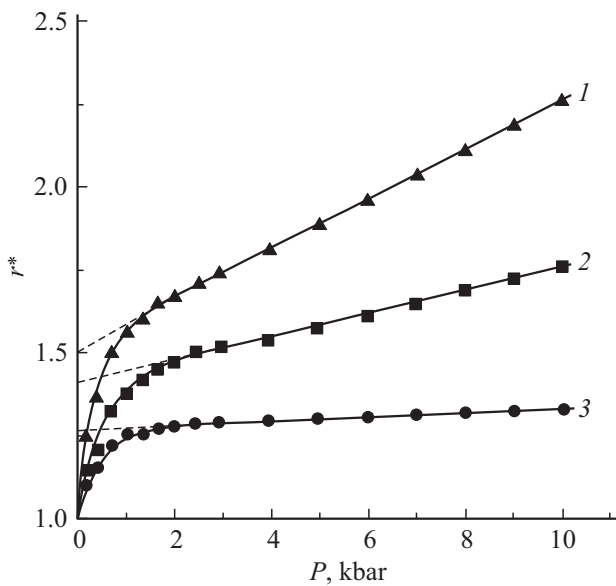


Figure 7. Integral polarization ratio for the photoluminescence band 1.18 eV in various *n*-GaAs:Te samples vs. uniaxial pressure along axis [111]. $T = 2$ K [37]. Electron concentration in samples n_0 , 10^{17} cm $^{-3}$: 1, 3 — 10, 2 — 5.

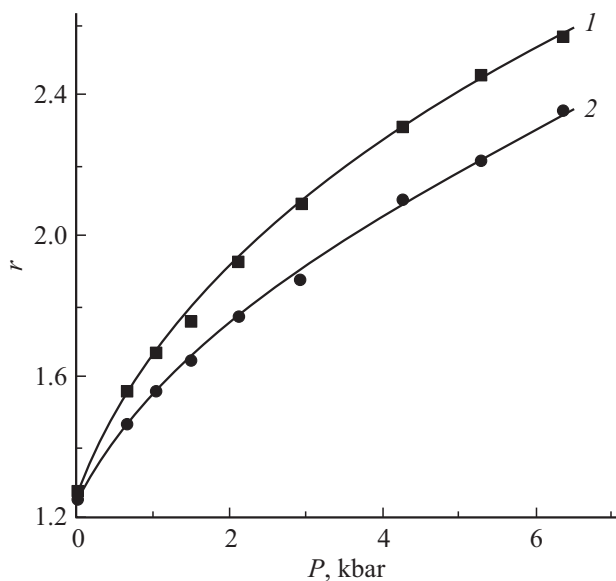


Figure 8. Polarization ratio of photoluminescence at photon energy $\hbar\omega_r = 1.2$ eV in different *n*-GaAs:Te samples vs. uniaxial pressure along axis [110] in case of polarized resonant excitation with photon energy $\hbar\omega_{ex} = 1.43$ eV. $T = 4.2$ K [37]. Experiment configuration $[001]-[\bar{1}10]$.

configurations appearance in the process of recombination through the complex of electron-hole pairs, similar to that observed under certain conditions for Jahn-Teller acceptors Cu and Au in GaAs [39].

Further studies [37] revealed that the dependences $r^* = f(P)$ of the studied band for different *n*-GaAs:Te crystals, have quantitative differences, although they retain

the above features (Fig. 7). Differences in the value r^* at $P \neq 0$ were also observed in the case of resonant polarized excitation (Fig. 8).

At the same time, at $P = 0$, the emission polarization under resonant polarized excitation for different samples remained practically the same within the experimental accuracy. This can be seen from Fig. 8, and for samples with different electron concentrations (n_0) it is shown in Fig. 9, which represents the values of the degree of linear polarization of photoluminescence ρ_1 and ρ_2 relative to the axis, perpendicular to the directions of propagation of the exciting and observed emission for $\eta = 0$ and experimental configurations $[110]-[001]$ and $[100]-[010]$, respectively.

Since in each experimental configuration with polarized resonant excitation, both $P = 0$ ρ_1 and ρ_2 are determined only by the parameters of the light emitting and absorbing dipoles (their direction in the local coordinate system associated with individual defect and the relative fraction of rotator and linear oscillator in the emission and absorption of light [30,32]), based on the above results it was supposed in the paper [37] that the photoluminescence band with a maximum of about 1.2 eV in *n*-GaAs:Te is caused by two types of centers, which are described by optical dipoles with similar parameters. Also, at low temperatures, the emission and absorption spectra of these centers are similar. However, distortions of centers of the first type are capable of changing orientation at low temperatures and aligning under the influence of relatively low pressures, while such

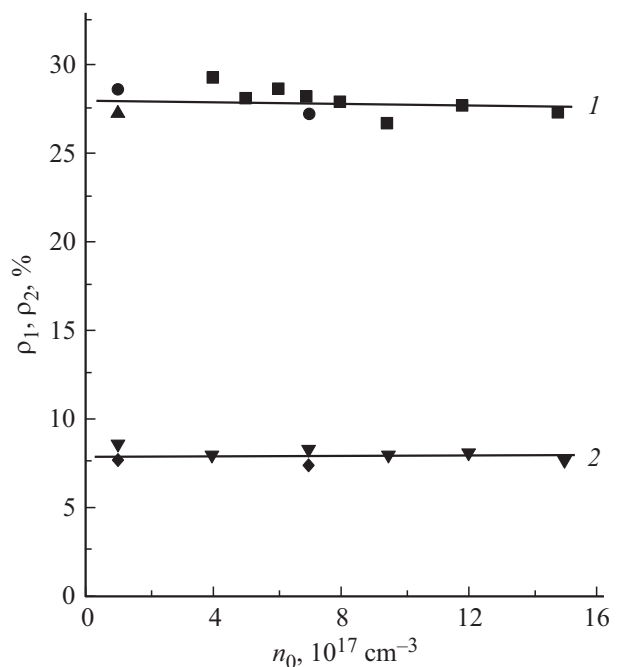


Figure 9. The degree of polarization of the 1.18 eV photoluminescence band in *n*-GaAs:Te samples with different electron concentrations upon resonant excitation by linearly polarized light with photon energy $\hbar\omega_{ex} = 1.43$ eV [37]. 1 — ρ_1 (experiment configuration $[1\bar{1}0]-[001]$), 2 — ρ_2 (experiment configuration $[100]-[010]$).

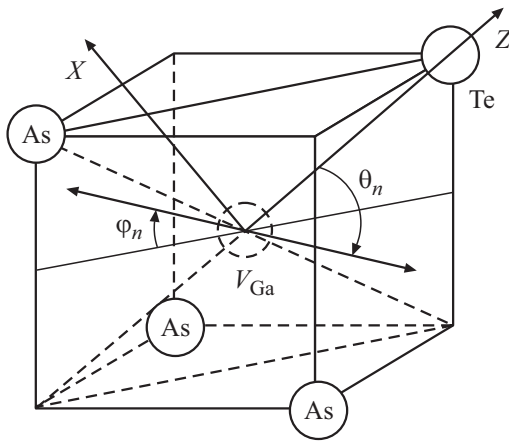


Figure 10. One of the possible configurations of $V_{Ga}Te_{As}$ complex with symmetry plane (110) and the direction of the optical dipole axis. X and Z — axes of the coordinate system introduced in Section 2.7.

reorientation and alignment do not occur in centers of the second type. The ratio of the concentrations of centers of these two types in different samples is different, which causes differences in the values of radiation polarization at uniaxial pressures.

The existence of reorientable Jahn-Teller distortions and the resulting monoclinic symmetry of the $V_{Ga}Te_{As}$ complex can be explained in the simplest model of the spatial structure of the complex, similar to the model of the vacancy — donor complex in Si, in which the reorientation and alignment of distortions caused due to the Jahn-Teller effect were observed using EPR [12,13]. In this model the distortion of the initial trigonal symmetry of the complex containing V_{Ga} , surrounded by three As atoms and Te_{As} atom at neighboring lattice sites, occurs in such a way, which preserves one of the symmetry planes of $\{110\}$ type containing Te_{As} , V_{Ga} and one of the three nearest atoms As (Fig. 10). For each complex there are three such planes and, consequently, three possible orientations of the Jahn-Teller distortion. In the case of complex distortion reorientation, its symmetry plane rotates around the axis $V_{Ga}-Te_{As}$. Thus, with equally probable distribution of Te_{As} over all possible places, the entire set of reorienting complexes $V_{Ga}Te_{As}$ in crystal at $P = 0$ will consist of 12 equally probable groups of complexes differing by various orientations of the symmetry plane of $\{011\}$ type.

Centers of the second type can be the same $V_{Ga}Te_{As}$ complexes, near which there is another shallow donor (Te_{As}) or other defect. As it was already mentioned in Section 1, the existence of associations of $V_{Ga}Te_{As}$ complex with an additional defect was assumed to qualitatively explain small variations in the parameters describing the photoluminescence band of these complexes in various n -GaAs:Te samples [21,22]. The electric or deformation field arising from the presence of additional defects can

stabilize one of the possible configurations of the complex (i.e., reduce its energy) and prevent the orientation change of its Jahn-Teller distortion at low temperatures and low uniaxial pressures. In this case, with pressure increasing a part of the complexes of the second type can pass into a configuration determined by the direction of pressure, but not by the direction of the field of the additional defect, i.e., the appearance of emission polarization of the entire set of complexes of the second type and increase in the total integral polarization of the photoluminescence band. Thus, the value r^* and the nature of its change with increasing pressure will be determined by the relative concentration of defects of the second type and the distribution of fields of additional defects in magnitude and direction. Both of these may depend on the conditions during crystal growth, and the difference in the $r^* = f(P)$ dependences for different samples may be due to this circumstance. (With equally probable distribution of additional defects of each type over possible places, all configurations of centers of the second type are equally probable, and at $P = 0$ the emission from the set of centers of the second type is also not polarized). Other reasons for r^* change at high pressures may be changes with pressure of the probability of alignment of second-type complexes during recombination [39]. In both cases, the extrapolation of the dependence $r^* = f(P)$ at relatively high pressures to $P = 0$ gives an estimate of r^* values, which is determined by the relative number of defects capable of reorienting in the external loads absence under experimental conditions.

2.3. Estimation of parameters of the emitting and absorbing dipoles of complex

The level splitting under the influence of internal uniaxial stresses used for calculating the degree of induced polarization (see Section 2.1), gives many options for the values of such splittings [34] and is not physically substantiated, although it allows one to establish the symmetry of the complex. A more illustrative picture is given by the description of the processes of emission and absorption of light by complex impurity centers by introducing classical optical dipoles [30–32].

In the general case, in this approximation each center is represented as a set of incoherent linear oscillator and rotator whose axes coincide, and frequencies differ by a very small amount. We will assume that the relative contribution of the rotator to the total emission (absorption) of the center is μ , and that of the linear oscillator, respectively, is $1-\mu$. In this case, as usual, the rotator can be represented by two mutually perpendicular coherent linear oscillators, the oscillation phase of which is shifted by 90° . Their contribution in the calculation of the intensity of emission (absorption) is averaged over time.

The estimate of the parameters of light absorbing and emitting dipoles of the complex in the model considered above was carried out in [37]. These dipoles in the

light emitting and absorbing states of the defect may differ due to, for example, lattice relaxation after the state change. Therefore, the two-dipole approximation was used to calculate the optical properties of such system. In [37] it was assumed that the dipoles of reorienting and non-reorienting complexes, in accordance with Section 2.2, are the same, and the dipole axis lies in the symmetry plane of the center. A similar preferred axis was observed in vacancy-donor complexes in Si and was identified mainly with a dangling bond of one of Si atoms [12]. The position of the axis can be characterized by the angle φ measured from the direction [110], which also lies in the plane of symmetry (Fig. 10). When light is absorbed, the optical dipole is described by the angle φ_1 and the contribution μ_1 , and when emitted — φ_2 and μ_2 , respectively [30,32], and the plane of symmetry of the center is preserved during the optical transition. At $P = 0$, reorienting and non-reorienting defects are optically indistinguishable and represent a single system.

The degree of the photoluminescence polarization of such system upon resonant excitation by light with electric vector perpendicular to the plane containing the directions of excitation and observation of photoluminescence, i.e., at $\eta = 0$, in the experimental configurations [110]–[001] and [100]–[010] respectively are equal

$$\rho_1 = \left[2a_1a_2(a_1a_2 + 4b_1b_2) \left(1 - \frac{3}{2}\mu_1\right) \left(1 - \frac{3}{2}\mu_2\right) \right] / R, \quad (4)$$

$$\rho_2 = \left[(3a_1^2 - 2)(3a_2^2 - 2) \left(1 - \frac{3}{2}\mu_1\right) \left(1 - \frac{3}{2}\mu_2\right) \right] / R, \quad (5)$$

where $a_{1,2} = \cos \varphi_{1,2}$, $b_{1,2} = \sin \varphi_{1,2}$,

$$R = \left[2 - \mu_1 - \left(1 - \frac{3}{2}\mu_1\right)a_1^2 \right] \left[2 - \mu_2 - \left(1 - \frac{3}{2}\mu_2\right)a_2^2 \right] + 2 \left[\mu_1 + \left(1 - \frac{3}{2}\mu_1\right)a_1^2 \right] \left[\mu_2 + \left(1 - \frac{3}{2}\mu_2\right)a_2^2 \right]. \quad (6)$$

In the case when the direction of the electric vector of the exciting light coincides with the direction of observation, i.e. $\eta = 90^\circ$, the emission is not polarized, which agrees with the experimental data (Fig. 4, *a, c*).

As it was already noted in Section 2.2, uniaxial pressure applied to the crystal causes alignment of Jahn-Teller distortions of reorienting complexes. In this case, as a result of alignment configurations begin to predominate in which the axis of the optical dipoles makes the smallest possible angle with the pressure axis. The integral value of the photoluminescence polarization of the system under study during the alignment of distortions and excitation due to the generation of electron-hole pairs by light from the intrinsic absorption band of GaAs will depend on the parameters of the emitting dipole and the number of defects, the distortions of which are capable of changing their orientation relative to the pressure axis. It is obvious

that at pressures close to 0, such defects are complexes that are not affected by additional defects located nearby, i.e., they are isolated. It can be assumed that the number of such defects for each group of complexes with different initial positions of the optical dipole axis relative to the pressure axis is the same due to the equally probable location of additional defects. The relative fraction of isolated complexes A determines the emission polarization at uniaxial pressures near 0. Since in the model under consideration (Fig. 10) in the region of high pressures the change in polarization is caused only by increase in the number of complexes capable of changing the orientation of distortions, this fraction can be related to the value of the integral polarization ratio obtained by extrapolating the experimental dependence $r_i^* = f(P)$ at high pressures to $P = 0$. In the case of pressure along the axis [110], when photoluminescence is excited due to the generation of electron-hole pairs by light from the intrinsic absorption band of GaAs, and the photoluminescence observation along the axis [1 $\bar{1}$ 0] or along the axis [001], respectively, these relations have the form

$$A \left(1 - \frac{3}{2}\mu_2\right) = \frac{8(r_{20}^* - 1)}{L - 2r_{20}^*(3b_2^2 - 1)}, \quad (7)$$

$$A \left(1 - \frac{3}{2}\mu_2\right) = \frac{8(r_{30}^* - 1)}{L + r_{30}^*(5a_2^2 + 6\sqrt{2}a_2b_2 + 2b_2^2)}, \quad (8)$$

where

$$L = 7a_2^2 + 6\sqrt{2}a_2b_2 - 2b_2^2, \quad (9)$$

r_{20}^* and r_{30}^* — extrapolated values of the polarization ratio at $P = 0$.

Since the measurements of r_2^* and r_3^* use the same sample in the form of a rectangular parallelepiped, the faces of which correspond to the planes (110), ($1\bar{1}$ 0) u (001), A for these measurements has the same value. Then, equating the right parts of equalities (7) and (8) to each other, we can obtain an equation for determining φ_2 . Substituting $r_{20}^* = 1.37$, $r_{30}^* = 1.95$ into this equation (Fig. 6) gives one of the solutions $\varphi_2 \approx 29^\circ$ (exact value $28^\circ 40'$). From equalities (7) and (8) one can also obtain the relation between μ_2 and the possible value A for the sample under study. At $\varphi_2 \approx 29^\circ$

$$\mu_2 \approx \frac{\frac{2}{3}(A - 0.32)}{A}. \quad (10)$$

Taking into account that, according to the definition μ_2 and A are positive and do not exceed 1, the relation (10) allows us to narrow the range of possible values of these parameters and establish that $0 \leq \mu_2 \leq 0.46$ and $0.32 \leq A \leq 1$.

The second solution $\varphi_2 \approx 145^\circ$ gives $A(1 - \frac{3}{2}\mu_2)$ more than 50, while by definition it must not exceed 1.

On the other hand, solving the system of equations (4) and (5) with respect to φ_1 and μ_1 and introducing the notation $c_{1,2} = \operatorname{tg} \varphi_{1,2}$, we can obtain

$$c_1 = \frac{2c_2 \pm \sqrt{4c_2^2 + \rho_1 \frac{(2c_2^2-1)}{\rho_2} \left[1 + \frac{\rho_1(2c_2^2-1)}{2\rho_2}\right]}}{\rho_1 \frac{(2c_2^2-1)}{\rho_2}}. \quad (11)$$

Substituting $\rho_1 = 0.28$, $\rho_2 = 0.08$ (Fig. 8) and $\varphi_2 \approx 29^\circ$ into (11) gives two values $\varphi_1 \approx -9^\circ$ and $\varphi_1 \approx -137^\circ$. Using these values of angle shows that only $\varphi_1 \approx -9^\circ$ satisfies the conditions $0 \leq \mu_1 \leq 1$, $0 \leq \mu_2 \leq 1$.

The results of the performed analysis show that the axes of the dipoles describing the absorption and emission of light differ noticeably and in both cases are strongly deviated from the direction of the trigonal axis connecting V_{Ga} and Te_{As} in the original position. Such behavior is associated with the Jahn-Teller effect existence of the static in the isolated complex.

On the other hand, it was found that the axis of the optical dipole in the emitting state deviates relatively weakly from the trigonal axis, which does not coincide with the original axis $V_{\text{Ga}}-\text{Te}_{\text{As}}$ for which $\varphi_2 \approx 35^\circ$. This causes relatively weak splitting of the energies of different configurations of the complex in the emitting state at pressure along the axis [100], which is observed experimentally (see Section 2.4).

The error in angles determination in the paper [30] is not specified. However, it follows from the estimates that if the relative error of r_{20}^*-1 and r_{30}^*-1 is $\pm 10\%$, the error φ_2 does not exceed $\pm 8^\circ$. Analysis of expressions (4) and (5) shows that the main error in the value φ_1 near the experimental values ρ_1 and ρ_2 is determined by the error φ_2 and is $\pm 11^\circ$.

The proximity of the emitting dipole axis to one of the directions $\langle 111 \rangle$, which does not coincide with the initial axis of the complex, is also confirmed by other experiments (Sections 2.4 and 2.6).

2.4. Analysis of the emission band at pressure along the axis [111]

As it is known (see, for example, [31,38]), uniaxial pressure splits the emission (absorption) band of anisotropic centers into several components corresponding to the emission (absorption) of groups of centers with different orientation relative to the pressure axis. The degree of polarization of each of these components is determined by the share of the rotator μ in the emitting (absorbing) dipole of the center and the angle between the axis of this dipole in the given group of centers and the pressure axis. However, in the case of a broad photoluminescence band the direct observation of individual components is impossible, and special methods must be used to distinguish them, based on various assumptions about the properties of the split components. One of such methods, based on measurements of photoluminescence spectra at

different orientations of the electric vector radiation ε_r with respect to the pressure axis, was proposed and implemented in [40].

The decomposition of broad band of emission into components is relatively easy to carry out if this band contains only 2 components. Such situation for monoclinic centers is realized at pressure along the axis [100] [38]. However, as experiments showed at $P \approx 8$ kbar [40], in this case the shape of the photoluminescence band is almost the same as the shape of the band at $P = 0$, and the splitting of the components with $\varepsilon_r \parallel P$ and $\varepsilon_r \perp P$ is small. This prevents a reliable decomposition of the measured emission band into components and is associated with the proximity of the axis of the emitting dipole to the direction of one of the axes $\langle 111 \rangle$ (Section 2.3), i.e. to the direction of the dipole in trigonal centers for which there is no splitting of the components for $P \parallel [100]$. Therefore, in paper [40] experiments were used under uniaxial pressure along the direction [111].

According to the considered model of the complex, such a pressure splits its emission band into three components corresponding to three groups of monoclinic centers with different orientations relative to the pressure axis. Different configurations in each group are equivalent with respect to the pressure axis, and the axes of their emitting dipoles lie in the plane of symmetry of the defect and are close to one of the directions $\langle 111 \rangle$, which do not coincide with the original axis $V_{\text{Ga}}-\text{Te}_{\text{As}}$. The first group is formed by complexes in which the pressure is directed along this axis. The axes of the emitting dipoles make a large angle with it. The second group includes complexes in which the pressure axis does not coincide with the original axis, but, as in the complexes of the first group, lies in the symmetry plane of the defect. The axes of the emitting dipoles of such complexes are close to the pressure direction (see Section 2.3 and Fig. 10). Complexes, in which the pressure axis does not lie in their plane of symmetry, form the third group. The axes of their emitting dipoles also make a large angle with the pressure axis.

Complexes of the second group at pressure have the lowest energy, and their number can increase with pressure increasing due to the rotation of the plane of symmetry of the third group complexes (i.e., „alignment“ of these centers). In complexes that have a stable configuration at $P = 0$ due to the influence of closely spaced defects, this occurs when the effect of pressure begins to exceed this influence.

The remaining unaligned part of the third group complexes should give the third emission component, since the angles between the axes of the dipoles and the direction of pressure, strictly speaking, differ from those in the first group.

The intensities of radiation Y_1, Y_2, Y_3 emitted in the direction $[1\bar{1}0]$ of each of these groups of complexes, in the case of photoluminescence caused by constant generation of electron-hole pairs, can be calculated in the dipole approach.

Expressions for them in relative units look like this:

$$Y_1(\parallel) = w_1 \left[(\sqrt{2}a_2 - b_2)^2 (1 - \mu_2) + (a_2 + \sqrt{2}b_2)^2 \frac{\mu_2}{2} \right], \quad (12)$$

$$Y_1(\perp) = \frac{1}{2} w_1 \left\{ (a_2 + \sqrt{2}b_2)^2 (1 - \mu_2) + [(\sqrt{2}a_2 - b_2)^2 + 3] \frac{\mu_2}{2} \right\}, \quad (13)$$

$$Y_2(\parallel) = 3w_2A^* \left[(\sqrt{2}a_2 + b_2)^2 (1 - \mu_2) + (a_2 - \sqrt{2}b_2)^2 \frac{\mu_2}{2} \right], \quad (14)$$

$$Y_2(\perp) = \frac{3}{2} w_2A^* \left\{ (a_2 - \sqrt{2}b_2)^2 (1 - \mu_2) + [(\sqrt{2}a_2 + b_2)^2 + 3] \frac{\mu_2}{2} \right\}, \quad (15)$$

$$Y_3(\parallel) = 3w_3(1 - A^*) \left[b_2^2(1 - \mu_2) + (a_2^2 + 2) \frac{\mu_2}{2} \right], \quad (16)$$

$$Y_3(\perp) = \frac{3}{2} w_3(1 - A^*) \left[(a_2^2 + 2)(1 - \mu_2) + (3 + b_2^2) \frac{\mu_2}{2} \right]. \quad (17)$$

Here A^* is the fraction of the second group complexes in the total number of defects of the second and third groups under the applied pressure, and w_1, w_2, w_3 are the relative fractions of the complexes of first, second and third groups captured the hole, i.e., being in the emitting state, under stationary conditions.

Since the axes of the dipoles in the third group, just as in the first group, are close to the axes $\langle 111 \rangle$, which do not coincide with the pressure direction, it can be assumed that the difference between the position of their emission bands at $P \parallel [111]$ is insignificant, and the total emission spectrum contains practically two components:

$$I_1 = Y_2, \quad (18)$$

$$I_2 = Y_1 + Y_3. \quad (19)$$

This circumstance was used to separate the components of the emission spectrum in the paper [40].

The experimental photoluminescence spectra associated with the $V_{\text{Ga}}\text{Te}_{\text{As}}$ complexes at pressure 10 kbar along the direction $[111]$ and temperature 2 K are presented in Fig. 11. It can be seen that the pressure caused a difference in the shifts of the spectra for different directions of the electric vector of the light wave, which indicates the splitting of the spectrum into several components belonging to different groups of centers. These components are not directly visible, and their separation from the total photoluminescence spectrum in each of the polarizations was based on the following simple assumptions.

1. The number of split components of the spectrum is equal to two.

2. The energy position of these components does not change when the plane of polarization of the registered

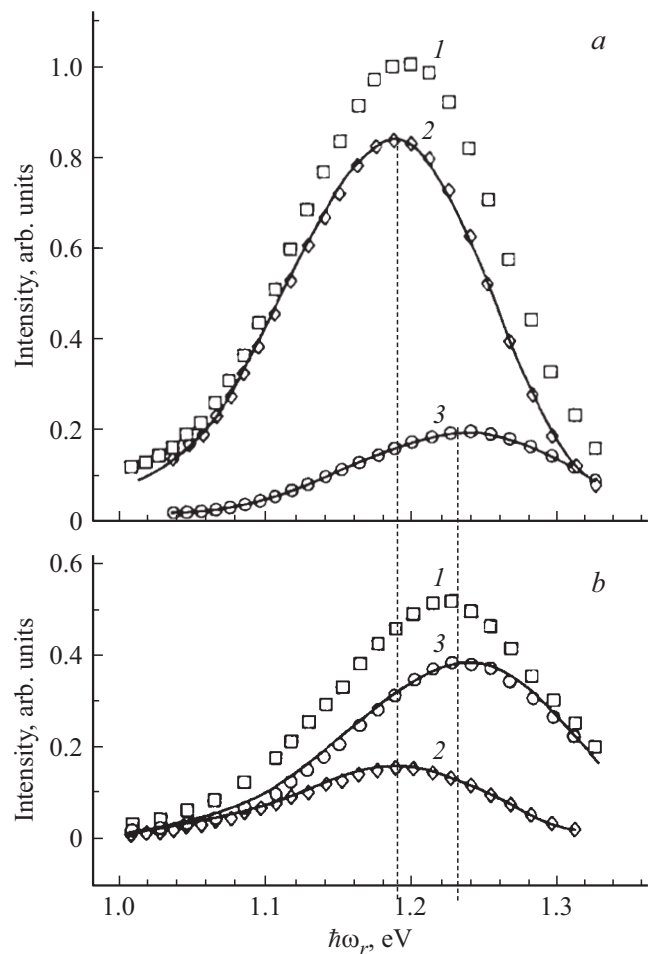


Figure 11. Photoluminescence spectra of $V_{\text{Ga}}\text{Te}_{\text{As}}$ complexes at temperature 2 K and pressure of 10 kbar along the direction $[111]$ [40]. $a - \epsilon_r \parallel P$, $b - \epsilon_r \perp P$. I — experiment, curves 2 and 3 — components 1 and 2 whose shape coincides with the shape of the photoluminescence spectrum at $P = 0$, points 2 and 3 — values of the photoluminescence intensities, which together give the experimental spectrum and best coincide with the curves 2 and 3.

emission changes, and the shape of their spectra is the same and coincides with the shape of the spectrum at $P = 0$, when there is no splitting of the components.

The results of such separation of the components are also shown in Fig. 11. The good coincidence achieved in this case between the total experimental emission spectrum in each of the polarizations and the total spectrum of components, the shape of which coincides with the shape of the spectrum when pressure is absent, shows that the splitting at pressure of the emission components associated with the first and third groups of complexes is small, which can indicate about the proximity of the axis of the emitting dipole of these configurations to the axes $\langle 111 \rangle$. The low-energy component I (Fig. 11) corresponds to complexes of the second group, in which the dipole axis is close to the pressure axis. The splitting of the components at $P = 10$ kbar is ~ 38 meV. The relative

values of their maxima for the electric radiation vector parallel and perpendicular to the pressure axis $I_{1\max}(\parallel)$, $I_{2\max}(\parallel)$, $I_{1\max}(\perp)$, $I_{2\max}(\perp)$, are ~ 0.85 , ~ 0.19 , ~ 0.15 , and ~ 0.385 , respectively.

When analyzing the results, it was assumed that the rates of capture of holes and electrons for defects of all groups at the applied pressure, as well as at $P = 0$, are the same, and therefore at low temperature $w_1 = w_2 = w_3$. Then, if we assume that the axis of the emitting dipole exactly corresponds to one of the directions of the type $\langle 111 \rangle$, which does not coincide with the original axis $V_{\text{Ga-TeAs}}$, it follows from expressions (12)–(19) that

$$\frac{I_1(\parallel)}{I_1(\perp)} = 2 \frac{1 - \mu_2}{\mu_2}, \quad (20)$$

$$\frac{I_2(\parallel)}{I_2(\perp)} = 2 \frac{1 + 3\mu_2}{8 - 3\mu_2}, \quad (21)$$

$$\frac{I_1(\parallel)}{I_2(\parallel)} = \frac{1 - \mu_2}{1 + 3\mu_2} \frac{27A^*}{4 - 3A^*}. \quad (22)$$

Since the shape of each of the spectrum components is the same, the ratios of the integral intensities in (20)–(22) can be replaced by the ratio of the values of each component at the emission maximum. Using their values, from (20) or (21) one can determine μ_2 , and from (22) — A^* . This gives $\mu_2 \approx 0.26$ and $A^* \approx 0.73$ (if all complexes are isolated, in the absence of distortions alignment, i.e. at $P = 0$ this value in the considered model is equal to $1/3$).

For $\varphi_2 \approx 29^\circ$ expressions (12)–(19) and the above results of spectrum decomposition in Fig. 11 give $\mu_2 \approx 0.25$ and $A^* \approx 0.75$.

2.5. Features of alignment of Jahn-Teller distortions of complex

The results of the experiments described in the previous Sections mean that at low temperatures and $P = 0$ the selective excitation of certain configurations of complexes, carried out using polarized resonant excitation, is accompanied by the preservation of the uneven distribution of the emitting state over all possible configurations for time exceeding the lifetime of this state τ_0 . This gives the observed photoluminescence polarization upon resonant polarized excitation. The absence of changes in the polarization diagrams of the complex with temperature increasing from 2 to 77 K [34] indicates that the characteristic reorientation time of the Jahn-Teller distortions of the emitting state even at 77 K in reorienting complexes significantly exceeds its lifetime, which, according to the results of paper [23], is relatively large (in $n\text{-GaAs:Te}$ samples with an electron density of $10^{17} - 10^{18} \text{ cm}^{-3}$, $\tau_0 \approx 10^{-6} \text{ s}$).

Such a situation, as shown in [41], persists at least up to temperatures $\sim 130 \text{ K}$ (Fig. 12) and is associated with a high barrier between equivalent configurations of individual complex in the emitting state, which prevents transitions from one configuration to another. At the same

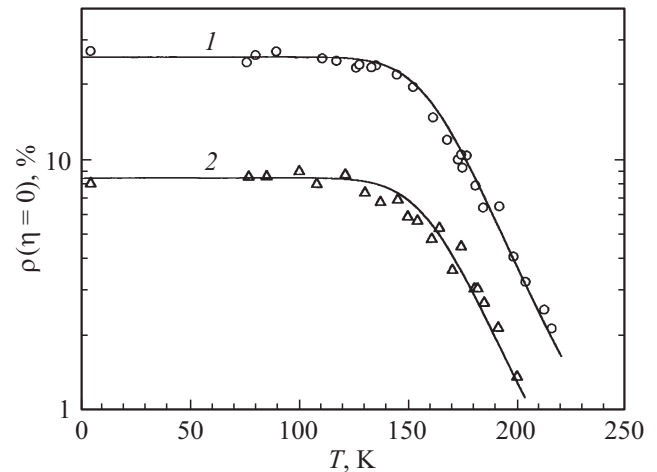


Figure 12. Degree of polarization of the photoluminescence band with maximum at photon energy of 1.18 eV in $n\text{-GaAs:Te}$ vs. temperature [41]. Polarized resonant excitation at $\hbar\omega_{\text{ex}} = 1.38 - 1.40 \text{ eV}$ and $\eta = 0$. Experimental configuration; 1 — $[110] - [001]$, 2 — $[100] - [001]$.

time, as follows from the study of the photoluminescence polarization at uniaxial pressures and interband excitation (Fig. 5–7), alignment of distortions of the emitting state occurs already at a temperature of 2 K. The totality of these facts means that under the influence of pressure, directly due to transitions between different configurations of the complex, only distortions in the absorbing state align, and this alignment is preserved when the complex is excited into the emitting state [41]. The stepwise nature of the polarization change with pressure increasing near $P = 0$ at temperature of 2 K and the strong polarization decreasing with temperature increasing to 77 K, observed during interband excitation (Fig. 6), indicate that the reorientation mechanism contains the thermal activation stage. In experiments on the influence of uniaxial pressure upon excitation of photoluminescence due to the generation of electron-hole pairs [35,36], the estimates show that the average time between the events of hole capture by a single center at 77 K did not exceed the lifetime of the emitting state by more than 2 orders of magnitude. This means that the barrier height in the absorbing state should be noticeably smaller than in the emitting state.

A similar stepwise increase in the polarization at 2 K and its disappearance at 77 K is also observed upon resonant excitation. This shows that the capture of holes from the valence band upon luminescence excitation by generating electron-hole pairs does not affect the reorientation (i.e., recombination-stimulated reorientation found for Au_{Ga} centers in GaAs [42], in the case of $V_{\text{Ga}}\text{TeAs}$ complexes does not play a significant role). Fig. 13 shows such a stepwise change in the induced polarization for pressure along the axis $[111]$, which, by aligning the distortions of the complexes in the absorbing state, increases the number of defects that are most effectively transferred to the emitting

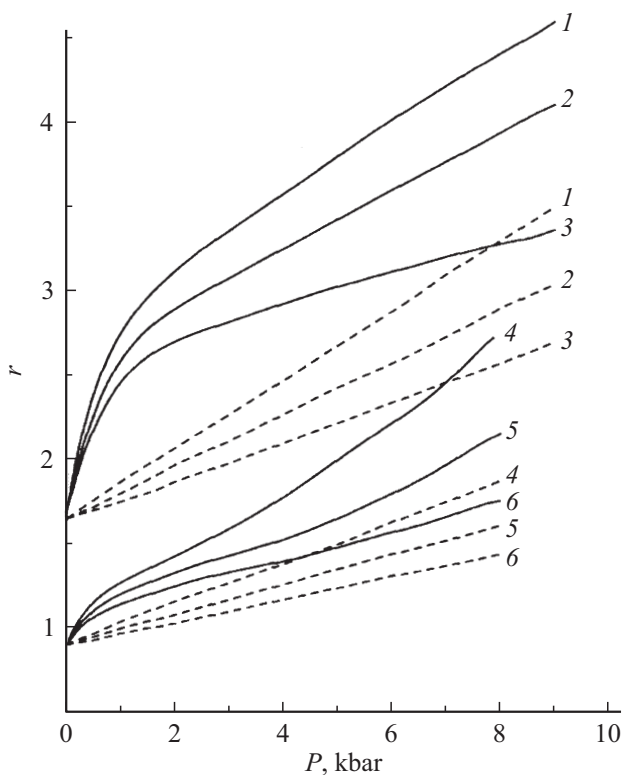


Figure 13. Polarization ratio of photoluminescence in the emission band $V_{\text{Ga}}\text{Te}_{\text{As}}$ under resonant polarized excitation as a function of pressure along the axis $[111]$ [41]. T, K : solid lines — 2, dashed lines — 77. 1–3 — $\eta = 0$, 4–6 — $\eta = 90^\circ$. $\hbar\omega_{\text{ex}}, \text{eV}$: 1, 4 — 1.40; 2, 5 — 1.43; 3, 6 — 1.46. $\hbar\omega_r \approx 1.2 \text{ eV}$. Configuration of excitation and observations of photoluminescence $[1\bar{1}0]-[11\bar{2}]$.

state during resonant excitation. The dependence of the polarization on the energy of exciting photons in this case is caused by the splitting of the energy levels of centers of different configurations under the influence of pressure.

The rapid decrease in the degree of induced polarization ρ under resonant polarized excitation and zero pressure in the case of high temperatures (Fig. 12) can be associated with a direct reorientation of distortions in the radiating state. In this case, the non-uniform distribution of the emitting state over all possible configurations of the complex decreases, and the absolute value of the induced polarization in the case of resonant polarized radiation should decrease. Another reason for the decreasing may be the thermal emission of holes from the emitting state of the complex into the valence band. Under stationary conditions, these holes are subsequently recaptured by complexes with any orientation of distortions and any direction of the original axis, transferring the complexes to the emitting state, which, with temperature increasing, leads to a more uniform distribution of this state over all possible configurations of the complex.

The analysis of the measurement results of this incidence in the one-dipole approximation [43] gave the conclusion

that the thermal emission of holes plays the main role. It was found that the activation energy of this emission is $\sim 170 \text{ meV}$. At the same time, estimates based on the possible values of the phonon energy of non-totally symmetric vibrations give the energy barrier for the re-orientation of distortions in the emitting state not lower than 200 meV , and this process can make a significant contribution to the dependence $\rho(T)$ at temperatures near 200 K and above [41,43].

2.6. Thermal redistribution of charge between complexes of different orientations and change in the polarization of their radiation during uniaxial deformation

If, as described in the previous Section, thermal emission of holes from complexes in the emitting state leads to the polarization decreasing of their emission under resonant polarized excitation at $P = 0$, then in the case of high uniaxial pressures, such emission can lead to increase in the integral polarization of emission.

Indeed, the external uniaxial deformation of the crystal violates the equivalence of anisotropic centers of the same type, which have different orientations with respect to the direction of deformation, and introduces various changes in the energy levels introduced by these centers into the forbidden band of the semiconductor. For centers with wide luminescence band, as the $V_{\text{Ga}}\text{Te}_{\text{As}}$ complexes we are considering, such levels splitting does not change the photoluminescence spectrum much, but it can lead to significant difference in energy activation of thermal emission of carriers from groups of centers of different orientations. As a result, under the conditions of photoluminescence observation under uniaxial deformation and temperature increasing, the rate of thermal emission of carriers captured by deep centers in the emitting state can reach the rate of radiative capture by these centers of carriers of the opposite sign and become higher than it for centers with a certain orientation relative to the deformation axis. Since, as already noted, the thermal ejection of carriers from these centers is accompanied by their recapture to centers of any orientation with equal probability, under stationary conditions, relatively more centers with orientation corresponding to the highest activation energy of the thermal emission of captured carriers will be in the emitting state. Such charge transfer from centers of one orientation to centers of another orientation leads to partial or complete elimination of the former from the radiative recombination process and change in the integral polarization of radiation in certain temperature range due to the appearance of a prevailing orientation of emitting recombination centers.

Since the energy level of the aligned at $P \parallel [111]$ complexes $V_{\text{Ga}}\text{Te}_{\text{As}}$, which give the polarization ratio increasing, in the emitting state is located closer to the bottom of the conduction band than for non-aligned ones (see Section 2.4), the described effect should lead to the

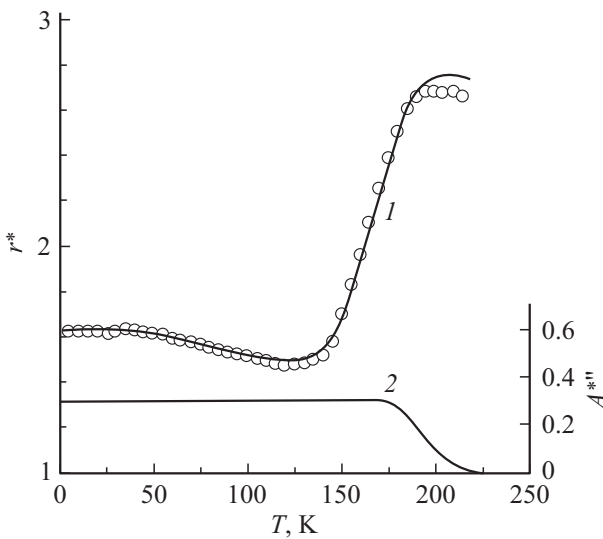


Figure 14. Temperature dependences of the integral polarization ratio of the 1.2 eV photoluminescence band in *n*-GaAs:Te at pressure of 10 kbar along the axis [111] (1) and the accepted during calculation share of non-restructuring complexes of the second group (2). Dots — experiment [44], curve — calculation at the values of the parameters specified in the text.

integral polarization increasing of emission with temperature increasing. This was observed in the paper [44] when photoluminescence was excited by the generation of electron-hole pairs, and emission was observed in the direction perpendicular to the pressure axis (Fig. 14).

Let us consider under these conditions the integral polarization of the emission band caused by the recombination of electron-hole pairs through the levels of the complexes under study, taking into account the thermal emission of holes in the emitting state. We will assume that the cross-sections for the capture of electrons and holes by the complex do not depend on the orientation of the original axis of the complex and its distortion with respect to the pressure axis.

At $P \parallel [111]$ the set of previously equivalent complexes is divided into 3 groups. In the first group, the original axis $V_{Ga}-Te_{As}$ coincides with the pressure axis, and there is no alignment of distortions under pressure. In the second and third groups, the complex configurations correspond to different directions of the dipole relative to the pressure axis and will have different energies. Since for the centers of these groups transitions from one group to another are possible simply due to the rotation of the plane of symmetry around the original axis of the complex (changes in the Jahn-Teller distortions orientation), alignment of centers can occur in the set of centers of the second and third groups. Adiabatic potentials W in the system of generalized coordinates Q associated with non-totally symmetric phonons, causing the Jahn-Teller effect, for set of complexes of the second and third groups and electron, which can be located both on the

complex and in allowed bands, at $P \parallel [111]$ are shown in Fig. 15.

The position of the energy levels of all groups of complexes in the emitting state relative to the edges of the allowed bands is shown in Fig. 16. The highest binding energy of holes in this state, which corresponds to the energy level E_2 (Fig. 16) ([37,40], Section 2.4), occurs in complexes of the group 2, in which the axis of the optical dipole is close to the pressure axis.

According to the conclusions of paper [41] (Section 2.5), a change in the direction of the individual center distortion

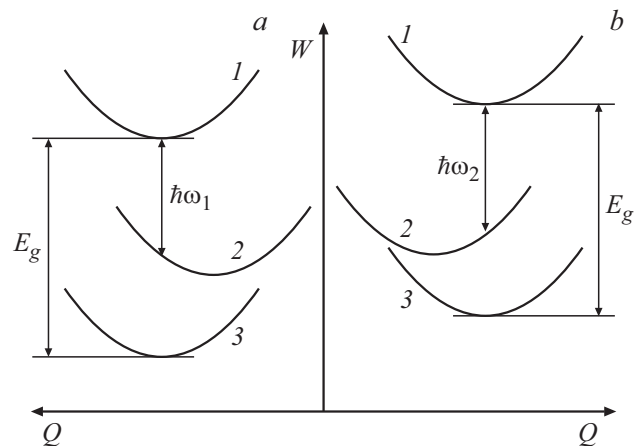


Figure 15. Scheme of adiabatic potentials (W) of the system electron + complex of the second (a) and third (b) groups in the space of generalized coordinates (Q) associated with non-totally symmetric oscillations at $P \parallel [111]$. 1 — electron at the bottom of the conduction band (emitting state), 2 — electron at the complex (absorbing state), 3 — electron at the top of the valence band.

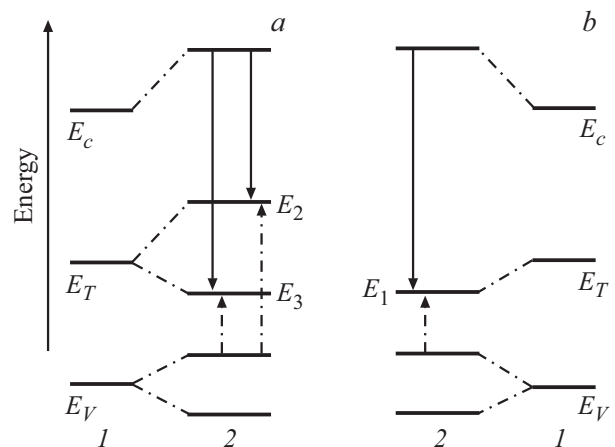


Figure 16. Schematic representation of the mutual arrangement of allowed band boundaries and energy levels of $V_{Ga}Te_{As}$ complexes in the emitting state in the absence of external pressure (1) and under uniaxial pressure along the axis [111] (2) [44]. a — complexes of the second and third groups, b — complexes of the first group. E_c , E_v and E_T , respectively, the energies of the bottom of the conduction band, the top of the valence band, and the level of complexes at $P = 0$. E_1 , E_2 and E_3 — energy levels of complexes of the first, second and third groups at pressure.

is possible only in the absorbing state, and the direction of the optical dipole axis in the emitting state is rigidly related to the direction of this dipole in the absorbing state. Let N_1, N_2 and N_3 be the total concentrations of defects of the first, second and third groups, the energy levels of which upon transition to the emitting state are E_1, E_2 and E_3 , respectively (Fig. 16), and p_1, p_2 and p_3 are the concentrations of the same defects already in the emitting state (i.e., in the state corresponding to localization of hole on the defect). Then, considering the capture and emission of holes and the capture of electrons, it is easy to show that in the stationary state under conditions of weak excitation of the luminescence of these defects ($p_1 \ll N_1, p_2 \ll N_2, p_3 \ll N_3$)

$$p_1 = \frac{C_p \tau_0 N_1}{1 + (1 - m) C_p \tau_0 N_v \exp\left(-\frac{E_1}{kT}\right)}, \quad (23)$$

$$p_2 = \frac{C_p \tau_0 N_2}{1 + (1 - m) C_p \tau_0 N_v \exp\left(-\frac{E_2}{kT}\right)}, \quad (24)$$

$$p_3 = \frac{C_p \tau_0 N_3}{1 + (1 - m) C_p \tau_0 N_v \exp\left(-\frac{E_3}{kT}\right)}. \quad (25)$$

Here C_p — coefficient of holes capture by centers, N_v — effective density of states of the valence band at uniaxial pressure, τ_0 — characteristic recombination time of holes at the center with electrons of conductivity band, m — the ratio of the rate of hole capture by complexes to the total rate of hole escape from the valence band due to capture by other deep centers and interband recombination [21,24,44]. N_1 does not change with pressure, and for equally possible distribution of original axes $V_{\text{Ga}}-\text{Te}_{\text{As}}$ is 1/4 of the total number complexes N . The remaining (3/4) N complexes are complexes of the second and third groups, i.e.

$$(3/4)N = N_2 + N_3. \quad (26)$$

If some of the complexes of these groups are capable of rearranging under pressure, the ratio between their equilibrium concentrations N'_2 and N'_3 will depend on the temperature

$$\frac{N'_3}{N'_2} = 2 \exp\left(-\frac{\Delta E'}{kT}\right), \quad (27)$$

where $\Delta E'$ is the difference between the energies of the complexes of the third and second groups in the absorbing state at uniaxial pressure along the direction [111].

The $\Delta E'$ value can noticeably differ from the analogous energy difference of these groups in the emitting state, however, at temperatures below ~ 40 K and $P = 10$ kbar it significantly exceeds kT . This is confirmed by the permanent integral polarization ratio in the specified temperature range (Fig. 14).

When calculating the total concentrations N_2 and N_3 , it should be taken into account that some part of these complexes N'_2 and N'_3 can be frozen and not rearrange at a

given pressure and temperature, i.e., the ratio between N'_2 and N'_3 is arbitrary.

The coefficients of proportionality relating the concentrations of centers N_1, N_2 and N_3 to p_1, p_2 and p_3 in expressions (23)–(25) are the relative emission probabilities w_1, w_2 and w_3 in the stationary state introduced earlier in expressions (12)–(17). The fraction of centers of the first group, as mentioned above, is constant and is taken into account in relative units in expressions (12) and (13). In the same relative units, using the parameter A^* , the fractions of the centers of the second and third groups are also taken into account: $A^* = (N'_2 + N'_3)/(N_2 + N_3)$. The total concentration of the centers of these groups, according to (26), should be preserved. The integral polarization ratio of the entire system of complexes at $P \parallel [111]$ was determined by the formula

$$r'_{111}(T) = \frac{Y_1(\parallel) + Y_2(\parallel) + Y_3(\parallel)}{Y_1(\perp) + Y_2(\perp) + Y_3(\perp)}. \quad (28)$$

To reduce the number of parameters describing the system, it was assumed [44] that

$$E_1 = E_3.$$

This assumption, as in Sections 2.4, was based on the proximity of the axes of the emitting dipoles of complexes with energies E_1 and E_3 to directions of the type $\langle 111 \rangle$ type, which do not coincide with the pressure axis [111], and, consequently, on the approximate equality of the angles between these axes and the direction of pressure for such centers.

During approximation of the experimental data (Fig. 14), in accordance with stated in Sections 2.3 it was assumed that $\mu_2 = 0.25, \varphi_2 = 28^\circ 40'$. The dependence of $C_p N_v \tau_0$ on temperature is not exactly known, because with temperature increasing N_v increases, and in the case of cascade and multiphonon capture mechanisms, the capture coefficient can drop sharply [45]. For simplicity, in the temperature range 125–215 K, where the thermal emission of holes from complexes becomes significant (Fig. 14), the value $C_p N_v \tau_0$ was assumed to be constant or decreasing. Pressure along the axis [111] equal to 10 kbar strongly splits the top of the valence band, significantly reducing the density of states at its top [46]. In the spherical approximation, the effective mass of the density of states M in this case is given by the relation

$$M^{3/2} = \frac{4m_h m_l}{3m_h + m_l} m_h^{1/2},$$

where m_h and m_l are the masses of heavy and light holes.

In accordance with this expression, N_v at high pressures will be ~ 0.19 of the values at $P = 0$.

The experimentally observed constancy of $r^*(T)$ at low temperatures also means that the exponential terms in (23)–(25) are small, i.e. $w_1 = w_2 = w_3$. Then from $r^*(2\text{ K})$ using relations (12)–(17) one can determine A^* . This makes it possible to obtain that in the

complex studied in [44] at $T = 2$ K the fraction of centers of the second group is $A^* \approx 0.6$, and the fraction of the third group is ~ 0.4 . The difference of A^* from 1 means that at low temperature all centers of the third group are frozen, while the fraction of frozen centers in the second group can be any. The further dependence of r^* on temperature can be described under various assumptions regarding the behavior of the centers of the second and third groups with temperature increasing. In this case, relations (26) and (27) must be satisfied.

Fig. 14 shows the results of the approximation under the assumption that some centers of the second group, whose fraction is $A''^* = N_2''/(N_2 + N_3) = 0.3$, remain unreconstructed up to 175 K, while the frozen number of centers of the third group remains unchanged over the entire temperature range studied. Such a difference in the behavior of frozen centers of different groups can be associated with differences in the position of the axes of their optical dipoles (i.e., the adiabatic potential minima where the center is located) relative to the pressure axis, as a result of which changes in the adiabatic potential near the center under the influence of pressures are different. The calculated curve was obtained for the following parameter values: $\Delta E' = 25$ meV, $E_1 = E_3 = 152$ meV, $E_2 = 190$ meV, $(1-m)C_p\tau_0N_v = 5 \cdot 10^4$, which remain unchanged in the temperature range 125–215 K. The change in the fracture of frozen centers of the second group is shown in Fig. 14.

Another possible assumption is that all the centers of the second group are not frozen already at 2 K, while the centers of the third group, frozen at low temperatures, with temperature increasing in the range 125–215 K gradually begin to be capable of reorientation under applied pressure or still remain frozen. In these cases, with a constant value $(1-m)C_p\tau_0N_v$ in the range $(5-3) \cdot 10^4$ and $\Delta E' = 27$ meV approximation of the experimental dependence $r^*(T)$ was achieved up to temperature of ~ 200 K. However, at $T = 215$ K the calculated value of $r^*(T)$ noticeably exceeded the experimental value. This discrepancy was eliminated by assuming that the value of $(1-m)C_p\tau_0N_v$ decreases with temperature increasing from 125 K, and in the temperature range 200–220 K is by 2–3 times lower than at 125 K.

In all cases, the integral polarization ratio decreasing in the temperature range up to 125 K is caused by increase in the concentration of centers of the third group with temperature increasing in accordance with relation (27), and its strong increasing at $T > 125$ K — with thermal emission of holes, leading to strong decrease in w_1 and w_3 relative to w_2 .

Also note that due to the high activation energies of the thermal emission of holes, the terms in the denominators of expressions (23)–(25), containing an exponent, at temperatures < 125 K are negligible at any reasonable values of $(1-m)C_p\tau_0N_v$. Because of this, the change in the pre-exponential multiplier in this temperature range is unimportant.

2.7. Model of complex $V_{Ga}Te_{As}$

As follows from the analysis of the experiments described in the previous Sections, the initially trigonal isolated complex, due to the Jahn-Teller effect, lowers its symmetry to monoclinic and has three equivalent configurations characterized by the existence of a plane of symmetry of $\{110\}$ type, which contains the original trigonal axis. In this case, the directions of the axes of the optical dipoles of the complex in the absorbing and emitting states differ strongly from each other and from the original trigonal axis of the complex. Spontaneous transitions of the complex from one equivalent configuration to another at helium temperatures are possible only in the absorbing state, while in the emitting state, during the lifetime of this state (about μs), such transitions are not observed, at least up to temperatures ~ 200 K (Section 2.5). The relation of these properties with each other, the charge state of the complex, and the parameters characterizing the influence of the donor and the Jahn-Teller effect can be understood from the review of the following model [47].

This model, as well as the model proposed for the qualitative interpretation of the properties of vacancy — donor complexes in Si [12,13], considers the originally trigonal complex distorted due to the interaction of electrons with not-totally symmetric vibrations; however, it assumes a another arrangement of one-electron energy levels at the center of C_{3v} symmetry. As in [12,13], the deepest level belongs to state of a_1 symmetry formed by the broken bond between the donor and the vacancy. The states with symmetry a_1 and e , formed by broken bonds of three As atoms surrounding the vacancy, have the sequence order opposite to that adopted in [13], i.e. level a_1 is located closer to the conduction band than the level e (Fig. 17, *a*). The strong interaction with the donor causes a significant distortion of the original wave functions of the vacancy (see, for example, [13]). In this case, the symmetry of the wave function of the upper a_1 state does not change, but the dipole matrix element of the optical transition of electron from the c -band to this state will differ significantly from the matrix element of the vacancy state. Interaction of electrons in two upper one-electron states (a_1 and e) with non-totally symmetric phonons of E -type [48] (Jahn-Teller pseudo-effect and Jahn-Teller effect) lead to further symmetry decreasing of the complex to monoclinic, to splitting of the electronic e -state, and a further change in the wave functions of electrons. In this case, as in [12,13], it can be assumed that the state a_1 with the deepest energy does not change under the influence of the electron-phonon interaction.

Considering the interaction of the original trigonal complex with E -vibrations in a cubic lattice, it is convenient to introduce a new rectangular coordinate system in which the axis Z coincides with the volume diagonal of the cube containing the donor, and axis X lies in the plane of symmetry of the monoclinic center (Fig. 10). The generalized coordinates of the E -vibrations associated with this system will be denoted by Q_x i Q_y . Then the Hamil-

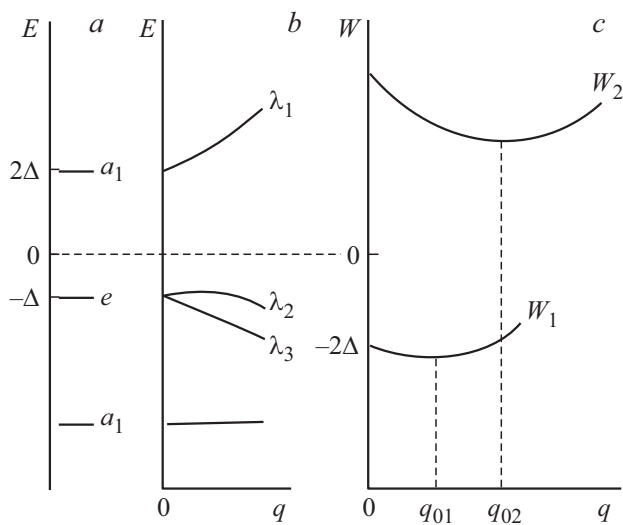


Figure 17. Scheme of electronic levels and adiabatic potentials of $V_{\text{Ga}}\text{Te}_{\text{As}}$ complex. *a* — scheme of electronic levels of the initial trigonal complex, *b* — one-electron energy levels vs. value of the generalized coordinate of vibrational motion q at $\beta = 0$, *c* — cross-section of adiabatic potentials at $\beta = 0$ for a system complex + 7 electrons in the absorbing and emitting states.

tonian describing the donor influence and the interaction of one electron with E -vibrations in the basis of the original vacancy wave functions X, Y, Z has the form

$$\hat{H} = \begin{pmatrix} -\Delta + F_2 Q_x & -F_2 Q_y & F_1 Q_x \\ -F_2 Q_y & -\Delta - F_2 Q_x & F_1 Q_y \\ F_1 Q_x & F_1 Q_y & 2\Delta \end{pmatrix}, \quad (29)$$

where 3Δ is the distance between the levels of the upper a_1 - and e -states without electron-phonon interaction, F_1 and F_2 are constants describing the Jahn-Teller pseudo-effect and effect, respectively. (Further in the text, for brevity, both effects will be referred to as JTE). Also note that in formula (29) and the subsequent expressions following from it, it is impossible to assume $\Delta = 0$, since in this case the symmetry of the complex is tetragonal, and the configuration of intrinsic vibrations of the atoms included in it is different. In the approximation of infinitely heavy nuclei, the wave functions Ψ_i and energies of one-electron states λ_i ($i = 1, 2, 3$) are determined from the equation

$$\hat{H}\Psi_i = \lambda_i\Psi_i. \quad (30)$$

With $Q_x, Q_y = 0$, $\lambda_2, \lambda_3 = -\Delta$, $\lambda_1 = 2\Delta$.

At $Q_x, Q_y \neq 0$ the expressions for λ_i become cumbersome, and further, for a qualitative consideration, we will use more simple expressions obtained under the condition that $F_1 \gg F_2$:

$$\lambda_1 = \frac{\Delta}{2} + \sqrt{\frac{9}{4}\Delta^2 + F_1^2 q^2} + \frac{F_1^2 F_2 q^3 \cos 3\beta}{2\left(\sqrt{\frac{9}{4}\Delta^2 + F_1^2 q^2} + \frac{3}{2}\Delta\right)\sqrt{\frac{9}{4}\Delta^2 + F_1^2 q^2}}, \quad (31)$$

$$\lambda_2 = \frac{\Delta}{2} - \sqrt{\frac{9}{4}\Delta^2 + F_1^2 q^2} + \frac{F_1^2 F_2 q^3 \cos 3\beta}{2\left(\sqrt{\frac{9}{4}\Delta^2 + F_1^2 q^2} - \frac{3}{2}\Delta\right)\sqrt{\frac{9}{4}\Delta^2 + F_1^2 q^2}}, \quad (32)$$

$$\lambda_3 = -\Delta - F_2 q \cos 3\beta, \quad (33)$$

where the designations $Q_x = q \cos \beta$, $Q_y = q \sin \beta$ are introduced, and the angle β is measured in the plane XY from the axis X .

In the absorbing state the vacancy complex binds 7 electrons,¹ two of which are at the deepest level, their energy makes a constant contribution to the energy of both absorbing and emitting states, and will not be taken into account in future. The remaining states, in which 5 electrons are located, change under the influence of JTE, and this must be taken into account when calculating the adiabatic potential of the center. Since $\lambda_1 + \lambda_2 + \lambda_3 = 0$, the total energy of these 5 electrons, neglecting the interaction between them compared to the influence of the donor and JTE [49], can be equal to $-\lambda_1, -\lambda_2$ or $-\lambda_3$. The minimum value of the total energy will be equal to $-\lambda_1$, i.e., under equilibrium conditions at low temperatures, there is one electron in the weakest bound state λ_1 . To determine the equilibrium configuration of the complex in the absorbing state, it is necessary to determine the position of the minimum of the adiabatic potential W_1 , which is equal to the sum of the total electron energy of 5 localized electrons and the energy of elastic vibrations (Fig. 17, c):

$$W_1 = -\lambda_1 + \frac{\kappa}{2} q^2, \quad (34)$$

where $\frac{\kappa}{2} q^2$ is the elastic energy of E -vibrations of atoms, κ is the elasticity coefficient. According to (34), in the space of generalized coordinates Q_x, Q_y at $F_2 = 0$ W_1 is independent of β and is an annular trough with radius q_{01} . At $0 < |F_2| \ll F_1$, 3 minima of the adiabatic potential appear on this trough, which correspond to $\beta = 0, 120$ and 240° at $F_2 > 0$.

In the emitting state 6 electrons are bound to the complex, and therefore only 4 electrons are localized in the considered upper states, and the fifth electron is in the conduction band. The minimum total electron energy of 5 electrons will be equal to $-2\lambda_1 + E_c$, where E_c is the electron energy in the c -band. In this case, the electronic state with energy λ_1 under equilibrium conditions at low temperatures is completely empty. In the emitting state, the adiabatic potential of the system complex + 5 electrons is (Fig. 17, c)

$$W_2 = -2\lambda_1 + \frac{\kappa}{2} q^2 + E_c. \quad (35)$$

Since the electron in the conduction band does not interact with E -vibrations, E_c does not depend on q , and

¹ This means that the complex in *n*-GaAs is singly ionized acceptor. The same conclusion was made in [1] on the basis of thermodynamic analysis of the degree of compensation of donors in GaAs grown under various conditions.

the form W_2 in the space of generalized coordinates of E -vibrations differs from (34) only by the coefficient 2 before λ_1 . As can be seen from (31), this is equivalent to replacing F_1, F_2 and Δ in (31) by $2F_1, 2F_2$ and 2Δ , respectively. Under the accepted condition $F_1 \gg F_2$, the value q_{0n} at the minimum of the adiabatic potentials of both states is determined by F_1 only:

$$q_{0n} = \frac{nF_1}{K} \sqrt{(1 - a_n^2)}, \quad (36)$$

where $n = 1$ or 2 respectively for an absorbing or emitting state,

$$a_n = \frac{3}{2n} \frac{\Delta}{F_1^2/K}. \quad (37)$$

As follows from (36) and (37), q_{02} noticeably exceeds q_{01} , i.e., the value of the Jahn-Teller distortion of the complex in the emitting state increases strongly (Fig. 17, *c*).

Under resonant excitation near the long-wavelength edge, electron transitions to the c -band occur precisely from the state λ_1 . The electron from the c -band passes into the same state during emission. However, the wave functions of this state at the minima of the adiabatic potential differ due to the difference in the complex distortion in the emitting and absorbing states. For $\beta = 0$

$$\Psi_n = \frac{1}{\sqrt{2}} \left(-\sqrt{1 - a_n} |X\rangle + \sqrt{1 + a_n} |Z\rangle \right). \quad (38)$$

For $a_n = 1$ the minimum of the adiabatic potential shifts to the point $q_{0n} = 0$, and for $a_n > 1$ expressions (36) and (38) are inapplicable (JTE is suppressed by the influence of the donor).

The wave functions of the state λ_1 in the other two configurations of the complex have the same form in similar coordinate system associated with the plane of symmetry of each configuration.

Transitions of electrons upon light absorption with photon energy near the long wavelength edge of the resonant absorption of light by the complex and subsequent emission occur between the state near the bottom of the conduction band, i.e., the s -type state and the state λ_1 with different center distortions. Then, by virtue of relation (38), the dipole matrix element of the transition has components along the axes X and Z . This means that the axes of the absorbing and emitting dipoles intersect with the initial axis of the trigonal center (axis Z) at angle θ_n (Fig. 10), which is measured from the axis Z towards the axis $-X$ and is determined by the relation

$$\theta_n = \arctg \sqrt{\frac{1 - a_n}{1 + a_n}} \frac{d_x}{d_z}, \quad (39)$$

where d_x is the projection onto the axis X of the dipole moment during optical transitions between the c -band and the initial e — state, and d_z — projection onto the axis Z of the dipole moment between the c -band and the initial a_1 -state. It can be seen from expression (39) that in the

emitting state due to a decreasing of a_n (expression (37)) θ_n should increase compared to absorbing state, which follows from the analysis of the experimental data.

The empirical model used in the analysis of the experimental data (see Section 2.3) assumed the existence, in addition to the linear oscillator, of a rotator incoherent with it. The considered model does not rely on such a representation. The introduction of the rotator can mean the existence in the absorption and emission of each configuration of the complex the set of differently directed component, linearly polarized in plane perpendicular to the axis of the main linear oscillator, i.e. in the plane XY . To approximate the polarization of the total light flux emitted by oscillators with this component in various experimental geometries, the effective rotator is introduced in the empirical model. The reasons for the occurrence of such a set may be different.

As noted earlier, a significant number of the studied centers are not reoriented due to the influence on such complex of other closely spaced local centers. Their influence can not only stabilize the individual type of configuration, but, if this additional defect does not lie in the same plane of symmetry of $\{110\}$ type, removes the axis of the linear oscillator out of this plane. (The symmetry of the system complex + additional defect decreases). The difference in the direction of these oscillator components occurs due to different positions of additional defects. Due to their incoherence, the polarization features associated with them are preserved in the total light flux measured in the direction chosen in the experiment. At the same time, due to the equally possible location of additional defects in all possible directions, the average direction of the axes of linear oscillators in set of such complexes corresponds to the axis specified by the minimum of the adiabatic potential of the isolated complex.

Another reason for such components occurrence is the atoms displacement in oscillatory motion, which plays a significant role for both non-reorienting and reorienting complexes. In other words, optical transitions go not only from the minimum of the adiabatic potential (AP), i.e., occur not only at q_{0n} and $\beta = 0, 120, 240^\circ$. At the moments of such transitions, the symmetry of the complex becomes lower than monoclinic. This leads to the occurrence of $|Y\rangle$ components in the electronic wave functions of the absorbing and emitting states. In different complexes and at different moments of time, when fast electron transitions occur, such displacements are different, which leads to the appearance of a set of differently directed linear oscillators during the time interval when measurements are made. Due to the symmetry of the probability distribution of atoms displacement with respect to the points q_{0n} and $\beta = 0, 120, 240^\circ$, the average direction of all linear oscillators in this case also corresponds to optical transitions in points of minimum of the adiabatic potential.

The value θ_n is related to the experimentally determined value φ_n by the relation $\theta_n = \varphi_n + \arctg \frac{1}{\sqrt{2}}$ and for the complex under consideration (see Section 2.3) is approxi-

mately equal to 27 and 64° in the absorbing and emitting states, respectively. Thus, to match the very simplified studied model with the data for the $V_{\text{Ga}}\text{Te}_{\text{As}}$ complex, it is necessary that in the absorbing state

$$\sqrt{1 - a_1 d_x} / \sqrt{1 + a_1 d_z} \approx 0.5,$$

and in the emitting state

$$\sqrt{1 - a_2 d_x} / \sqrt{1 + a_2 d_z} \approx 2.$$

In the limit of strong JTE for the emitting state $a_2 \rightarrow 0$ and the minimum value of the ratio $d_x/d_z \approx 2$. Since in the considered model this relation is also preserved during absorption, this means that in the absorbing state $a_1 \approx 0.9$. If in the emitting state a_2 differs from 0, $d_x/d_z > 2$ and in the absorbing state a_1 increases, but remains < 1 , i.e. distortion of the complex due to EJT is preserved.

The JTE decreasing in the absorbing state following from the considered model can explain the low-temperature reorientation of the equivalent configurations of the complex in the absorbing state, and the absence of such reorientation in the emitting state up to temperatures ~ 200 K. Indeed, at not too high temperatures in thermal equilibrium, the complex distortion in the emitting and absorbing states corresponds to one of the equivalent minima of the adiabatic potential, which, according to expressions (31), (36) and (37), are separated by energy barrier ΔW_n

$$\Delta W_n = \frac{F_1 F_2}{K} n^2 \frac{[1 - (a_n)^2]^{3/2}}{1 + a_n/2}. \quad (40)$$

As can be seen from expression (40), the barrier height in the emitting state, according to expressions (31), (36) and (37), significantly exceeds that in the absorbing state. Also note that the barrier between equivalent configurations can additionally increase with change in the number of electrons per level due to the existence of quadratic terms of the Jahn-Teller interaction [49].

A characteristic feature of the emission polarization behavior of the complexes under study in the case of pressure along the axis [001] is a slight difference in the integral polarization ratio at temperatures of 2 and 77 K, i.e., a weak effect of the degree of distortions alignment on the emission polarization (Fig. 5). As with other pressure directions, distortions alignment occurs due to reorientation in the absorbing state. In this state, there are 2 groups of configurations with different angles between the pressure axis and the directions of the optical dipole axes, and therefore a noticeable alignment at 2 K should take place even at low pressures, as it is observed for pressure directions along the axis [111] or [110]. However, in any of the existing groups of configurations, the axis of the emitting dipole is close to the direction of the axis of the [111] type, and due to the equally probable Te distribution in the complex over all possible positions in any of the groups all directions of the emitting dipoles are equally probable. If the axis of the emitting dipole exactly coincides with one

of the axes [111], the emission polarization in the case of pressure along the axis [001] would be absent even with complete alignment of the distortions. Since there is no such coincidence, and there is a small difference in the deviation of the emitting dipole axis from the [111] type axis for different configurations, a small increase in the photoluminescence polarization at helium temperatures (i.e., with increase in the degree of alignment) occurs.

Thus, the considered model qualitatively at the microscopic level describes well the main optical properties of the $V_{\text{Ga}}\text{Te}_{\text{As}}$ complexes and their relation to each other.

Previously, in the paper [50], not a trigonal center, but a vacancy surrounded by 4 As atoms, was assumed as the original model of the complex. The interaction of electrons in such a tetrahedral complex with *F*-vibrations gives 4 equivalent minima of the adiabatic potential corresponding to the trigonal distortion of the defect. The effect of the donor was assumed to be weaker and changed the equivalence of these minima in such a way that the minimum energy is in those 3 configurations of the complex which original distortion axis did not coincide with the vacancy — donor axis. However, a detailed consideration, similar to the given above, showed that in this case it is not possible to obtain the change in the directions of the absorbing and emitting dipoles indicated in Section 2.3.

3. Complexes $V_{\text{Ga}}\text{S}_{\text{As}}$

As already noted in the Introduction, the GaAs photoluminescence band, which is characteristic for the emission of gallium vacancy — donor complexes, was also observed in a material doped with other elements of the VI group, namely, Se and S [14,15]. However, fewer works related to the study of these defect properties. For $V_{\text{Ga}}\text{Se}_{\text{As}}$ complexes, only emission spectra at temperature of 74 K and excitation by light from the intrinsic absorption region of GaAs were published [14,15]. The $V_{\text{Ga}}\text{S}_{\text{As}}$ complex was studied in more detail by piezospectroscopic methods [50–52]. Next, we consider the results of these studies.

3.1. Piezospectroscopic studies of the 1.2 eV emission band in *n*-GaAs : S

Early studies of the emission band of $V_{\text{Ga}}\text{S}_{\text{As}}$ complexes in *n*-GaAs:S at temperatures 2 and 77 K [50,51] found that the behavior of the polarization of the emitted light at uniaxial pressures along [111] and [001] directions differs markedly from the behavior of the photoluminescence of the $V_{\text{Ga}}\text{Te}_{\text{As}}$ complexes. It turned out that, although the symmetry of the complexes is lower than trigonal, there is no any alignment of additional distortions of the complexes under conditions of uniaxial deformation at low temperatures. A more detailed study was carried out in [52] and confirmed these conclusions. Fig. 18, *a, b* shows the emission spectra of the $V_{\text{Ga}}\text{S}_{\text{As}}$ complexes in the absence of deformation and for uniaxial pressure along [001]

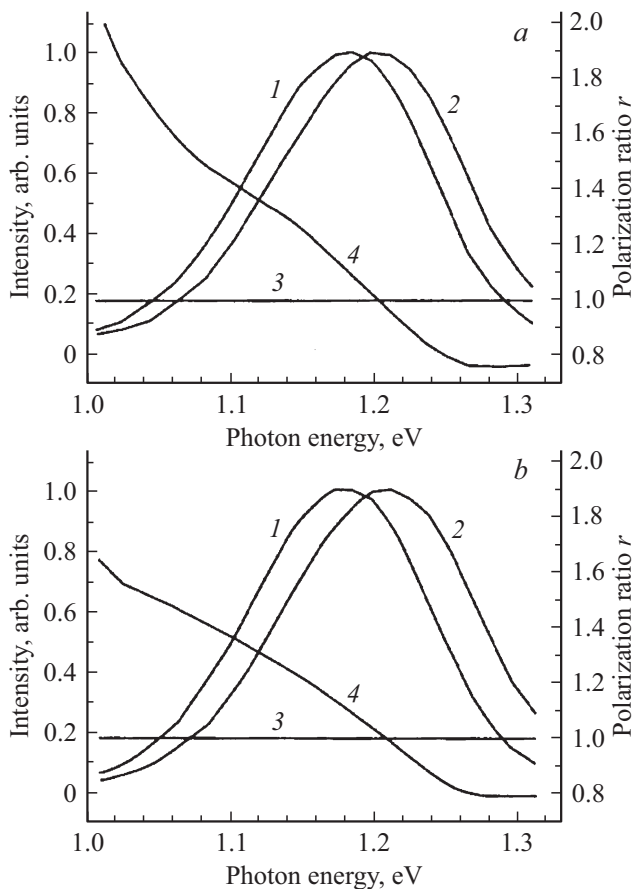


Figure 18. Spectral distribution of photoluminescence intensity (I , 2) and its polarization ratio r (3, 4) of $V_{\text{Ga}}\text{S}_{\text{As}}$ for $P = 0$ (1, 3) and $P = 8$ kbar (2, 4) [52]. a — $P \parallel [001]$, b — $P \parallel [111]$.

and $[111]$ directions, as well as the spectral distribution of the pressure-induced linear polarization r of the emitted light [52]. The photoluminescence excitation was caused by the generation of electron-hole pairs by light from the intrinsic absorption band of GaAs. (The measurement geometry corresponds to Fig. 1, b , temperature 2 K). It is seen, that the uniaxial pressure in both directions somewhat broadens and noticeably shifts the emission band, and also leads to a very different polarization of light in different parts of its spectrum. In this case, as the measurements showed, the integral polarization ratio for the entire band r^* is equal to 1. Such a change in the emission characteristics is typical for the splitting of the emission band into components corresponding to different orientations of the complex configurations relative to the axis of external deformation, and indicates that all configurations are excited with equal probability, and their symmetry is not higher than monoclinic with the plane of symmetry of the $\{011\}$ type [31]. Since the dispersion of the polarization ratio at pressures along the axes $[111]$ and $[001]$ does not differ much, it can be assumed that the axis of the

emitting dipole is approximately equally deviated from the directions $\langle 001 \rangle$ and $\langle 111 \rangle$, lying in the same plane with it.

The dependences of the pressure-induced integrated polarization of the emission band on temperature are shown in Fig. 19. Within the measurement accuracy, the integral polarization ratio r_{001}^* and r_{111}^* remains equal to 1 up to temperature of ~ 50 K, and then, in the entire measured temperature range (up to 150 K) it increases for both directions of external deformation. (At higher temperatures the intensity of the emission band becomes too low and measurements of the integrated polarization were not carried out). This growth is not caused by the alignment of additional distortions of the complexes, but is a consequence of the thermal ejection of holes from centers of that orientation, the energy level of which in the emitting state at uniaxial pressure becomes closest to the top of the valence band (the activation energy of thermal emission of holes from complexes in this configuration becomes the lowest). This phenomenon was also observed for the $V_{\text{Ga}}\text{Te}_{\text{As}}$ complexes and considered in Section 2.6. However, for $V_{\text{Ga}}\text{Te}_{\text{As}}$ such growth occurs only for $P \parallel [111]$ (Fig. 19). The existence of a strong increase in the integral polarization with temperature increasing for $V_{\text{Ga}}\text{S}_{\text{As}}$ both for $P \parallel [111]$ and for $P \parallel [001]$ is explained by the significant splitting of the emission components in both cases, which confirms the data in Fig. 18. As follows from this figure, it is the low-energy component of the emission, which arises due to electron transitions to energy levels closest to the conduction band, that has a polarization ratio greater than 1.

3.2. Structure of the center and parameters of the emitting dipole

The highest possible monoclinic symmetry of the initially trigonal complex $V_{\text{Ga}}\text{S}_{\text{As}}$ is similar to the symmetry of the complex $V_{\text{Ga}}\text{Te}_{\text{As}}$, i.e. for each of the possible positions of the initial trigonal axis $V_{\text{Ga}}-\text{S}_{\text{As}}$, 3 equivalent configurations with $\{011\}$ plane of symmetry containing this axis must exist. If we assume that just this symmetry is realized, and there is no alignment of distortions, then at uniaxial pressures along the $[111]$ or $[001]$ directions the emission band in the set of such defects should split into 3 and 2 components, respectively [38].

Separation of these components in the emission band of the $V_{\text{Ga}}\text{S}_{\text{As}}$ complex upon equally probable excitation of all configurations due to the generation of electron-hole pairs in the simpler case $P \parallel [001]$ was implemented in the paper [52]. In the classical dipole approximation, assuming, as in the case of the $V_{\text{Ga}}\text{Te}_{\text{As}}$ complex, that the axis of the emitting dipole is in the plane of symmetry of the defect (Fig. 10), and the emission observation direction is perpendicular to the pressure axis $[001]$, one can obtain the following relations between the intensities of the split

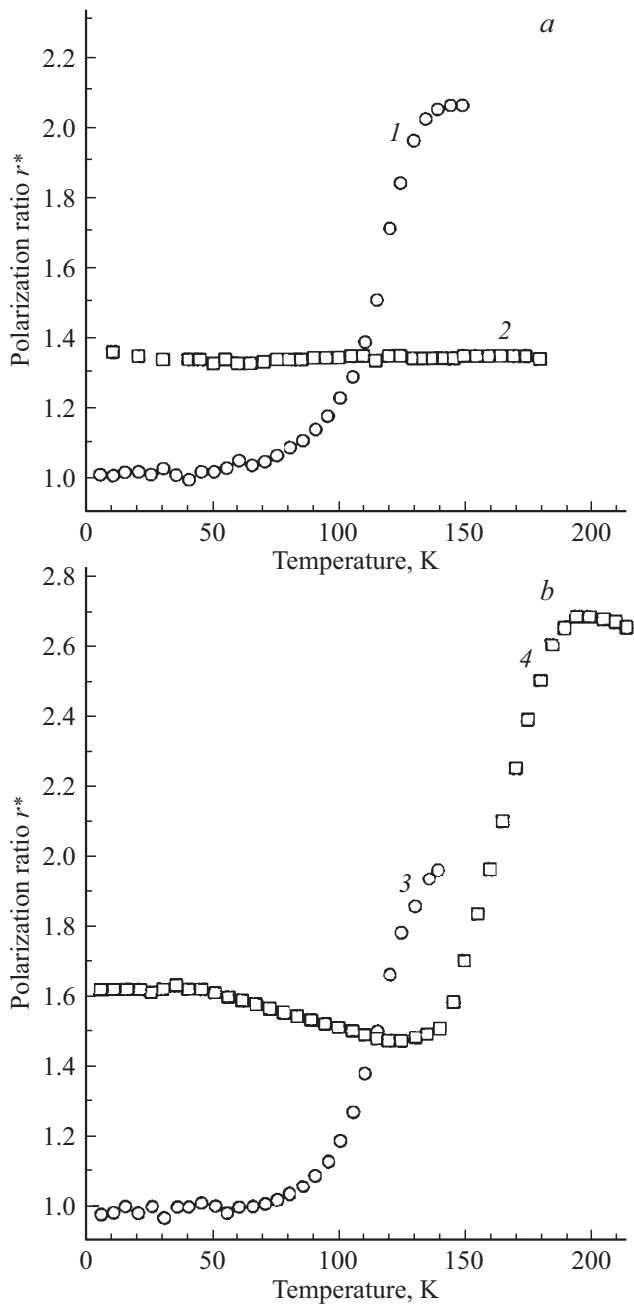


Figure 19. Integral polarization ratio of photoluminescence r^* of $V_{\text{Ga}}\text{S}_{\text{As}}$ and $V_{\text{Ga}}\text{Te}_{\text{As}}$ complexes at uniaxial pressure vs. temperature [52]. *a* — $P \parallel [001]$, *b* — $P \parallel [111]$. 1, 3 — $V_{\text{Ga}}\text{S}_{\text{As}}$, 2, 4 — $V_{\text{Ga}}\text{Te}_{\text{As}}$, 1–3 — $P = 8$ kbar, 4 — $P = 10$ kbar.

components of the radiation band in different polarizations:

$$I_1(\parallel) = I_1(\perp) \left[\mu_2 + 2b_2^2 \left(1 - \frac{3}{2} \mu_2 \right) \right] / \left[\mu_2 + a_2^2 \left(1 - \frac{3}{2} \mu_2 \right) \right], \quad (41)$$

$$I_2(\parallel) = 2I_1(\perp), \quad (42)$$

$$I_2(\perp) = I_1(\parallel) + I_1(\perp). \quad (43)$$

Here $I_1(\parallel)$, $I_1(\perp)$, $I_2(\parallel)$, $I_2(\perp)$ are respectively the total intensities of the first and second photoluminescence com-

ponents in the cases when the electric vector of the light wave is parallel or perpendicular to the pressure axis; μ_2 , a_2 and b_2 — parameters of the emitting dipole of the $V_{\text{Ga}}\text{S}_{\text{As}}$ complex, similar to the parameters introduced in Section 2.3 for the complex $V_{\text{Ga}}\text{Te}_{\text{As}}$.

Since at low temperatures the integral polarization of the band under study does not arise up to pressures of 8 kbar (Fig. 19, *a*), it can be assumed that the effect of such a pressure is reduced only to a different change in the energy levels of defects with different orientation, and does not change their electronic wave functions. In this case, the spectral shape of each of the split components repeats the shape of the spectrum in the absence of deformation, and the total intensities of these components in expressions (41)–(43) can be replaced by the intensities at the maximum of each component.

As was identified in [52], the decomposition of the photoluminescence band at $P \parallel [001]$ into two components, taking into account the above conditions and relations (42) and (43), is possible, and its results are presented on Fig. 20. At that the position of the maxima in the spectra of the components corresponds to $\hbar\omega_1 \approx 1.188$ eV, $\hbar\omega_2 \approx 1220$ eV (splitting of the components (32 ± 4) meV), and the relative value of the emission intensity at the maxima of the components is $I_{1\text{max}}(\parallel) = 0.82$ – 0.81 , $I_{1\text{max}}(\perp) = 0.09$ – 0.10 , $I_{2\text{max}}(\parallel) = 0.18$ – 0.20 , $I_{2\text{max}}(\perp) = 0.92$ – 0.91 .

The decomposition into two components of the spectra at $P \parallel [111]$ turned out to be impossible, which was expected for the emission of monoclinic centers with $\{011\}$ plane of symmetry, which in principle split into 3 components in this case.

Separation of the components of the luminescence spectra at $P \parallel [001]$ and determination of their polarization makes it possible to estimate the possible parameters of the emitting dipole of the complex. Indeed, it follows from relation (41) that

$$a_2^2 = \cos^2 \varphi_2 = [2 - \mu_2(\gamma + 2)] / \left[\left(1 - \frac{3}{2} \mu_2 \right) (\gamma + 2) \right], \quad (44)$$

where $\gamma = I_{1\text{max}}(\parallel) / I_{1\text{max}}(\perp)$.

Since $\gamma = 8$ – 9 , and the values of the dipole parameters are limited by definition: $0 \leq \mu_2 \leq 1$ and $0 \leq \cos^2 \varphi_2 \leq 1$, relation (44), as numerical calculations show, is satisfied only at $0 \leq \mu_2 \leq 0.2$. At that, if $\mu_2 = 0.2$, $\varphi_2 = \pm 90^\circ$, i.e., the axis of the optical dipole in any configuration of the complex, parallel to the axis $\langle 001 \rangle$, which lies in the plane of symmetry of the configuration (Fig. 10). μ_2 decreasing leads to $|\varphi_2|$ monotonous decreasing to $\sim 63^\circ$ at $\mu_2 = 0$.

To narrow the ranges of possible values of these parameters of the emitting dipole, one can use experimental data on the increase in polarization due to thermal emission of holes $P \parallel [111]$ (Fig. 19, *b*). First of all, note that at $\varphi_2 = \pm 90^\circ$, according to the expressions (12)–(17) applicable to this case, the emission of each of the three groups of centers is not polarized. In this case, the observed polarization increasing with temperature increasing cannot occur either

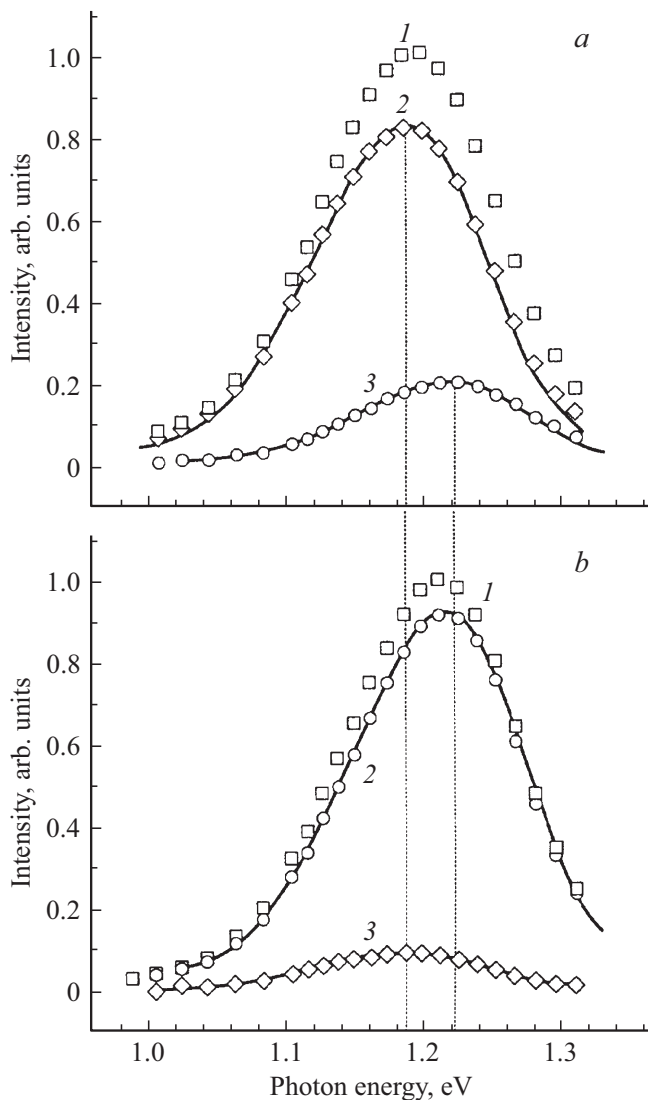


Figure 20. Photoluminescence spectra of $V_{\text{Ga}}\text{S}_{\text{As}}$ complexes and their components at different polarizations of the detected emission and pressure 8 kbar along the direction [001]. $T = 2\text{ K}$ [52]. a — $\varepsilon_r \parallel P$, b — $\varepsilon_r \perp P$. 1 — experimental spectrum at pressure, curves $2, 3$ — components whose shape coincides with the shape of the spectrum at $P = 0$, dots $2, 3$ — emission intensities, which together give the experimental spectrum and best coincide with the curves $2, 3$.

due to alignment of distortions or due to a change in the relative probabilities of the existence of emitting state in each group of complexes due to thermal emission of holes. Hence $|\varphi_2| < 90^\circ$ and $\mu_2 < 0.2$. Numerical analysis of expressions (12)–(17) when relation (44) is satisfied shows that in the case of $\varphi_2 > 0$ only the second group of complexes has a polarization ratio r greater than 1, and the first and third groups have $r < 1$. If $\varphi_2 < 0$, then $r > 1$ only for the first group, while for the second and third groups $r < 1$.

As can be seen from Fig. 19, b , increase in the integral polarization ratio for the entire emission band with tem-

perature increasing at pressure of 8 kbar occurs at least up to ~ 2.1 and, possibly, even more. From this, taking into account the above, it follows that the group that makes the prevailing contribution to the integral polarization of the entire emission band at $P \parallel [111]$ should have $r > 2.1$. Calculations using expressions (12)–(15) and (44) show that this condition is achieved in both cases, if $0 \leq \mu_2 \leq 0.15$, and hence $63 \leq \varphi_2 \leq 75^\circ$ or $-63 \geq \varphi_2 \geq -75^\circ$.

Thus, the piezospectroscopic behavior of the photoluminescence band $V_{\text{Ga}}\text{S}_{\text{As}}$ agrees with the model of monoclinic defect with $\{011\}$ plane of symmetry. The axis of the emitting optical dipole of this complex lies in the plane of its symmetry and is strongly deviated from directions of $\langle 111 \rangle$ and $\langle 001 \rangle$ types, which lie in the same plane.

4. Conclusion

The presented results of studies of complexes formed in n -GaAs by gallium vacancy and atom of element of VI group of Periodic System Te or S, replacing As atom in the lattice site adjacent to the vacancy, show that their symmetry is below trigonal, and their optical properties are explained in the model of monoclinic defect, which has $\{011\}$ plane of symmetry, containing the original trigonal axis. The reason for such symmetry decreasing is the interaction of electrons localized at the center with incompletely symmetric vibrations (the Jahn-Teller effect).

In case of $V_{\text{Ga}}\text{Te}_{\text{As}}$ the directions of the axes of the optical dipole in the absorbing and emitting states are very different. In this case, the axis of the emitting dipole is close to the axis of $\langle 111 \rangle$ type, which does not coincide with the original axis $V_{\text{Ga}}-\text{T}_{\text{As}}$. At low temperatures, a relatively fast spontaneous reorientation of the isolated complex is possible, i.e., its transition to another equivalent configuration due to rotation of the plane of symmetry around the original axis. This leads to alignment of complexes under uniaxial deformation. The existence of additional defects near some of the complexes can lead to the stabilization of a certain configuration of the complex. A feature of such complexes alignment is the possibility of overcoming the stabilizing effect of additional defect at sufficiently high uniaxial deformations. The latter at low temperatures causes a gradual increase in the photoluminescence polarization of complexes with increase in uniaxial deformation, which follows a stepwise increase at small deformations associated with the alignment of isolated centers. The number and location of these additional defects in different samples may vary, which causes a difference in the dependence of the emission polarization on the uniaxial pressure. In this case, as it was shown by studies of the photoluminescence of samples with different concentrations of Te under resonant polarized excitation, the parameters of optical dipoles, which characterize the entire set of complexes in the sample, practically do not change. The reorientation of the complex occurs only in the absorbing state and, upon transition to the emitting state, the position

of the plane of symmetry is preserved. The direction of the axes of optical dipoles in the absorbing and emitting states differs greatly due to the change in the number of electrons captured by the center. These properties of $V_{\text{Ga}}\text{Te}_{\text{As}}$ are explained in the model of original trigonal complex, in which the one-electron state involved in optical transitions has a_1 symmetry. Symmetry decreasing in this state is only possible due to the Jahn-Teller pseudo-effect when mixed with the e -state due to the interaction with the only non-totally symmetric vibration of the E -type, which exists in trigonal complex containing 4 atoms.

For $V_{\text{Ga}}\text{S}_{\text{As}}$ complexes the photoluminescence studies were carried out only when it was excited by light from the intrinsic absorption band of GaAs. Unlike the $V_{\text{Ga}}\text{Te}_{\text{As}}$ complex the distortions $V_{\text{Ga}}\text{S}_{\text{As}}$ do not reorient and do not align at uniaxial pressures up to 10 kbar even at high temperatures, and the deviation of the axis of the emitting optical dipole from directions of the $\langle 111 \rangle$ and $\langle 001 \rangle$ types in the plane of symmetry of the complex is approximately the same. May be, as it was suggested in the paper [52], this is associated with the displacement of the atom S_{As} in the tetrahedral environment of atoms Ga not along the $[111]$ axis, as happens in the case of Te_{As} , but along the $[001]$ axis, and with the formation of Ga–Ga dimer whose axis is perpendicular to the plane of symmetry of the defect predicted by DX-center calculation [53,54]. If such changes are realized in the $V_{\text{Ga}}\text{S}_{\text{As}}$ complex, the position of the plane of symmetry of the complex is additionally stabilized, and reorientation becomes more difficult. However, the presence of V_{Ga} in the environment of S atom changes the situation greatly, since in the initial state the environment becomes trigonal and a broken bond appears. To substantiate this possibility, detailed calculations of the complexes themselves are required, which are currently not available. Another possibility is to change the values of the constants of the Jahn-Teller electron-phonon interaction, which results in the mixing of all one-electron vacancy states. Then, as the initial defect, it is necessary to consider V_{Ga} , the symmetry of the environment of which is decreased due to interaction with non-totally symmetric vibrations of the tetrahedral complex. In this case, if in the complex $V_{\text{Ga}}\text{S}_{\text{As}}$ the interaction with E -vibrations dominates, the direction of the optical dipole axis in the emitting state may be closer to the direction of $\langle 001 \rangle$ type than in the case of the complex $V_{\text{Ga}}\text{Te}_{\text{As}}$. This possibility also requires detailing of the model and calculations.

Conflict of interest

The authors declare that they have no conflict of interest.

References

- [1] D.T.J. Hurle. *J. Appl. Phys.*, **107**, 121301 (2010).
- [2] Filip Tuomisto, Ilja Makkonen. *Rev. Mod. Phys.*, **85**, 1583 (2013).
- [3] Christoph Freysoldt, Blazej Grabowski, Tilmann Hickel, Jörg Neugebauer, Georg Kresse, Anderson Janotti, Chris G. Van de Walle. *Rev. Mod. Phys.*, **86**, 253 (2014).
- [4] Fumiyasu Oba. *Proc. AIP*, **1763**, 040003 (2016).
- [5] Joseph C.A. Prentice, Bartomeu Monserrat, R.J. Needs. *Phys. Rev. B*, **95**, 014108 (2017).
- [6] J.S. Prener, F.E. Williams. *J. Chem. Phys.*, **25**, 261 (1956).
- [7] D. Curie, J.S. Prener. In *Physics and Chemistry of II–VI Compounds*, ed. by M. Aven and J.S. Prener (North-Holland Publishing Co., Amsterdam, 1967) p. 445.
- [8] T. Koda, S. Shionoya. *Phys. Rev.*, **136**, A541 (1964).
- [9] J. Schneider, A. Rauber, B. Dischler, T.L. Estle, W.C. Holton. *J. Chem. Phys.*, **42**, 1839 (1965).
- [10] G.D. Watkins, J.W. Corbett. R.M. Walker. *J. Appl. Phys.*, **30**, 1198 (1959).
- [11] E. Sonder, L.C. Templeton. *J. Appl. Phys.*, **34**, 3295 (1963).
- [12] G.D. Watkins, J.W. Corbett. *Phys. Rev.*, **134**, A1359 (1964).
- [13] E.L. Elkin, G.D. Watkins. *Phys. Rev.*, **174**, 881 (1968).
- [14] E.W. Williams. *Phys. Rev.*, **168**, 922 (1968).
- [15] E.W. Williams, H.B. Bebb. In *Semiconductors and Semimetals*, ed. by R.K. Willardson and A.C. Beer (Academic Press, N.Y.–London, 1972) v. 8, p. 321.
- [16] M.B. Panish, H.J. Queisser, L. Derick, S. Sumski. *Solid State Electron.*, **9**, 311 (1966).
- [17] H.J. Queisser, C.S. Fuller. *J. Appl. Phys.*, **37**, 4895 (1966).
- [18] J.S. Prener, D.J. Weil. *J. Electrochem. Soc.*, **106**, 409 (1959).
- [19] E.W. Williams, A.M. White. *Solid State Commun.*, **9**, 279 (1971).
- [20] K.D. Glinchuk, A.V. Prokhorovich, V.I. Vovnenko. *Phys. Status Solidi A*, **34**, 777 (1976).
- [21] V.I. Vovnenko, K.D. Glinchuk, A.V. Prokhorovich. *Sov. Phys. Semicond.*, **10**, 652 (1976).
- [22] V.I. Vovnenko, K.D. Glinchuk, A.V. Prokhorovich. *Sov. Phys. Semicond.*, **10**, 1227 (1976).
- [23] K.D. Glinchuk, A.V. Prokhorovich, V.E. Rodionov. *Sov. Phys. Semicond.*, **11**, 18 (1977).
- [24] K.D. Glinchuk, A.V. Prokhorovich. *Phys. Status Solidi A*, **44**, 777 (1977).
- [25] V.I. Vovnenko, K.D. Glinchuk, K. Lukat, A.V. Prokhorovich. *Sov. Phys. Semicond.*, **14**, 596 (1980).
- [26] D.T.J. Hurle. *J. Phys. Chem. Solids*, **40**, 627 (1979).
- [27] D.T.J. Hurle. *J. Phys. Chem. Solids*, **40**, 639 (1979).
- [28] J.E. Stehr, K.M. Johansen, T.S. Bjørheim, L. Vines, B.G. Svensson, W.M. Chen, I.A. Buyanova. *Phys. Rev. Appl.*, **2**, 021001 (2014).
- [29] Mykhailo Vorobiov, Oleksandr Andrieiev, Denis O. Demchenko, Michael A. Reshchikov. *Phys. Rev. B*, **104**, 245203 (2021).
- [30] P.P. Feofilov. *Polyarizovannaya lyuminesentsiya atomov, molekul i kristallov* (M., Gos. izd-vo fiz.-mat. lit., 1959). (in Russian)
- [31] P.P. Feofilov, A.A. Kaplyanskii. *Sov. Phys. Usp.*, **5**, 79 (1962).
- [32] E.E. Bukke, I.N. Grigoriev, M.V. Fok. *Tr. FIAN*, **79**, 108 (1974). (in Russian)
- [33] I.A. Buyanova, S.S. Ostapenko, M.K. Sheinkman. *Sov. Phys. Solid State*, **27**, 461 (1985).
- [34] N.S. Averkiev, A.A. Gutkin, E.B. Osipov, M.A. Reshchikov, V.E. Sedov, V.R. Sosnovskij. *Sov. Phys. Semicond.*, **25**, 28 (1991).
- [35] N.S. Averkiev, A.A. Gutkin, E.B. Osipov, M.A. Reshchikov, V.E. Sedov, V.R. Sosnovskij. *Sov. Phys. Semicond.*, **25**, 33 (1991).

- [36] N.S. Averkiev, A.A. Gutkin, E.B. Osipov, M.A. Reshchikov, V.E. Sedov, V.R. Sosnovskij. *Sov. Phys. Semicond.*, **26**, 708 (1992).
- [37] A.A. Gutkin, M.A. Reshchikov, V.E. Sedov. *Semiconductors*, **34**, 1151 (2000).
- [38] A.A. Kaplyanskii. *J. de Phys.*, **28** (Suppl. 8–9), 4 (1967).
- [39] A.A. Gutkin, N.S. Averkiev. *Semiconductors*, **51**, 1247 (2017).
- [40] A.A. Gutkin, A.V. Ermakova. *Semiconductors*, **37**, 884 (2003).
- [41] A.A. Gutkin, M.A. Reshchikov, V.E. Sedov. *Zeitschrift für Physikalische Chem.*, **200**, 217 (1997).
- [42] N.S. Averkiev, T.K. Ashirov, A.A. Gutkin, E.B. Osipov, V.E. Sedov, A.F. Tsatsulnikov. *Sov. Phys. Semicond.*, **25**, 1134 (1991).
- [43] A.A. Gutkin, M.A. Reshchikov, V.E. Sedov. *Semiconductors*, **31**, 908 (1997).
- [44] A.A. Gutkin, M.A. Reshchikov. *Semiconductors*, **37**, 271 (2003).
- [45] V.N. Abakumov, V.I. Perel', I.N. Yassievich. *Bezizluchatel'naya rekombinatsiya v poluprovodnikakh* (SPb, Ioffe FTI RAN, 1997). (in Russian)
- [46] R.N. Bhargava, M.I. Nathan. *Phys. Rev.*, **161**, 695 (1967).
- [47] N.S. Averkiev, A.A. Gutkin. *Tez. dokl. XV Ross. konf. po fizike poluprovodnikov* (N. Novgorod, 3–7 oktyabrya, 2022.) p. 225. (in Russian)
- [48] I.B. Bersuker. *The Jahn-Teller Effect* (UK, Cambridge, Cambridge University Press, 2006).
- [49] N.S. Averkiev, A.A. Gutkin, M.A. Reshchikov. *Semiconductors*, **29**, 624 (1995).
- [50] A.A. Gutkin, N.S. Averkiev, M.A. Reshchikov, V.E. Sedov. *Proc. 18th Int. Conf. on Defects in Semicond.* (Sendai, Japan, July 23–28, 1995), ed. by M. Suezawa and H. Katayama-Yoshida [*Mater. Sci. Forum*, **196–201** (1), 231 (1995)].
- [51] A. Gutkin, M. Reshchikov, V. Sedov, V. Sosnovskij. *Proc. Estonian Acad. Sci. Phys. Math.*, **44** (2/3), 212 (1995).
- [52] A.A. Gutkin, M.A. Reshchikov. *Semiconductors*, **38**, 791 (2004).
- [53] D.J. Chadi, C.H. Park. *Proc. 18th Int. Conf. on Defects in Semicond.* (Sendai, Japan, July 23–28, 1995), ed. by M. Suezawa and H. Katayama-Yoshida [*Mater. Sci. Forum*, **196–201** (1), 285 (1995)].
- [54] C.H. Park, D.J. Chadi. *Phys. Rev. B*, **54**, 14246 (1996).